National and Kapodistrian University of Athens

Oceanography and Management of Marine Environment

Specialization: Chemical Oceanography

A Dissertation for the Degree of Master of Science in Oceanography and Management of Marine Environment

Decadal/Multidecadal palaeoceanographic variability in the Saronikos Gulf during the Holocene: climatic conditions and human pressures

Alexandros Papaioannou

Advisory Committee:

Prof. Maria Triantaphyllou

Prof. Manos Dasenakis

Dr Alexandra Gogou

Athens, 2019

Acknowledgements

I would like to thank my advisory committee, Prof. Maria Triantaphyllou, Prof. Manos Dasenakis and Dr Alexandra Gogou for their continuous support. I would also like to express my deepest gratitude to Dr Constantine Parinos who supported me through the whole experimental process in HCMR, for his overall support and guidance, as well as for his constructive comments on this thesis, and Prof. Katerina Kouli for her guidance, and Mr. Costas Miaritis for providing valuable pollen data from the same core that helped me to interpret my thesis findings. I would further like to thank Dr Ioannis Hatzianestis and Dr Alexandra Pavlidou who provided me the opportunity to have access to the biogeochemical laboratory and research facilities at the HCMR and for providing me with the sea surface temperature data of Elefsis Bay for the last 20 years.

In addition, I would like to thank Elvira Plakidi and Stella Chourdaki, organic chemists, for their help in the lab.

Finally, I would like to express my gratitude towards my family and my girlfriend, who supported and encouraged me during this thesis.

Athens, A. Papaioannou

October 2019

Abstract

The present study focuses on the identification of land-sea climate interactions, the sensitivities and response modes of the marine environment to temperature and hydrological changes and the human pressures during the last 300 years in the Elefsis Bay. The study area is located next to metropolitan area of Athens, having as a consequence high inputs of organic material. The approach adopted here uses selected marine and terrestrially derived biogeochemical indices retrieved from the WF-S2 sedimentary record. These lipid biomarkers carry a specific signal from the environment in which they were synthesized. Thus, they can be used at reconstructing past sea surface temperatures (SSTs), organic matter inputs, marine productivity, upwelling intensity, soil inputs, changes in land vegetation and precipitation patterns etc. The organic compounds identified in WF-S2 multi-core were *n*-alkanes, *n*-alkanols, long chain alkenones, sterols and polycyclic aromatic hydrocarbons (PAHs). The core can be divided into two different periods, the pre-industrial and the industrial one. During the pre-industrial period, which lasts until the last decades of the 19th century, the various biomarkers show periods with higher supply from continental/riverine runoffs and consequently significant terrestrial inputs and other more stable periods. Also through the study of various proxies (PAHs, coprostanol etc.) the enlargement of the settlements of the surrounding area and the increased wood burning are obvious from the beginning of the 19th century. After the onset of the industrial period the rise of the population of the surrounding area and the overall enhanced inputs of anthropogenic hydrocarbons are evident through an increased export of terrestrial organic matter of biogenic and anthropogenic origin to the marine environment. The further study of PAHs identifies their signal as a mixed contribution, mainly from pyrolytic sources and secondary of unburned fossil fuels, as deduced from their molecular profile and source-specific indices. At the same time, an increase in all marine markers is recorded, which can be attributed to the enhanced supply of terrigenous matter and the concomitant supply of nutrients to the core site.

Περίληψη

Η παρούσα εργασία στοχεύει αναγνώριση των αλληλεπιδράσεων ξηράς-θάλασσας, στις ευαισθησίες και στην απόκριση του θαλάσσιου περιβάλλοντος στις θερμοκρασιακές και υδρολογικές αλλαγές, καθώς και στις ανθρωπογενείς πιέσεις που δέχεται ο κόλπος της Ελευσίνας κατά τη διάρκεια των τελευταίων 300 χρόνων. Η περιοχή μελέτης βρίσκεται δίπλα στην ευρύτερη μητροπολιτική περιοχή της Αθήνας, έχοντας ως επακόλουθο την εισροή μεγάλων ποσοτήτων οργανικού υλικού στο θαλάσσιο περιβάλλον. Για τη μελέτη των παραπάνω χρησιμοποιήθηκε μια σειρά από επιλεγμένους βιογεωχημικούς δείκτες (θαλάσσιας και χερσαίας προέλευσης), με το ίζημα να προέρχεται από τον πυρήνα WF-S2. Αυτοί οι βιοδείκτες προέρχονται από λιπίδια και μπορούν να χρησιμοποιηθούν ώστε να γίνει ανάπλαση παλαιών επιφανειακών θερμοκρασιών (SSTs), εισροών οργανικού υλικού, πρωτογενούς παραγωγικότητας, χερσαιοπαροχής, ανάδυσης υδάτων (upwelling), αλλαγών στη βλάστηση κλπ. Οι οργανικές ενώσεις που χρησιμοποιήθηκαν ως βιοδείκτες ανήκουν στις ομάδες *κ*-αλκάνια, *κ*-αλκανόλες, αλκενόνες, στερόλες και πολυκυκλικούς αρωματικούς υδρογονάνθρακες (PAHs). Ο πυρήνας WF-S2 μπορεί χωριστεί σε δύο περιόδους, την προ-βιομηχανική περίοδο και την βιομηχανική. Η προ-βιομηχανική περίοδος διαρκεί μέχρι τις τελευταίες δεκαετίες του 19ου αιώνα. Κατά τη διάρκεια της, η ανάλυση διαφόρων βιοδεικτών δείχνει περιόδους με υψηλότερη παροχή από τη χέρσο ή τα ποτάμια και άλλες περιόδους με πιο ήπιες συνθήκες. Επίσης, συγκεκριμένοι δείκτες (PAH, κοπροστανόλη κλπ.) αποκαλύπτουν τη διεύρυνση των παρακείμενων οικισμών και την αυξημένη καύση ξύλου ήδη από τις αρχές του 19ου αιώνα. Με το ξεκίνημα της βιομηχανικής εποχής φαίνεται ξεκάθαρα η ραγδαία αύξηση του πληθυσμού στις γειτονικές περιοχές καθώς και η μεγάλη παροχή ανθρωπογενών υδρογονανθράκων στο θαλάσσιο περιβάλλον. Μελετώντας περαιτέρω τις κατανομές των πολυκυκλικών αρωματικών υδρογονάνθρακων (PAHs), διαπιστώθηκε ότι είναι κυρίως προϊόντα πυρολυτικής προέλευσης (διεργασίες καύσης) και δευτερευόντως εναποθέσεις άκαυστων πετρελαιοειδών.

Contents

List of Figures

List of Tables

1 INTRODUCTION

According to Intergovernmental Panel on Climate Change (IPCC), the global climate has been constantly warming during the last decades, which is mainly associated with the anthropogenic greenhouse gases [1]. The current levels of greenhouse gases are unprecedented in at least 800,000 years. Concentrations of carbon dioxide (CO_2), methane (CH_4) and nitrous oxide (N_2O) have all shown large increases since the beginning of the Industrial Era (Figure 1.1).

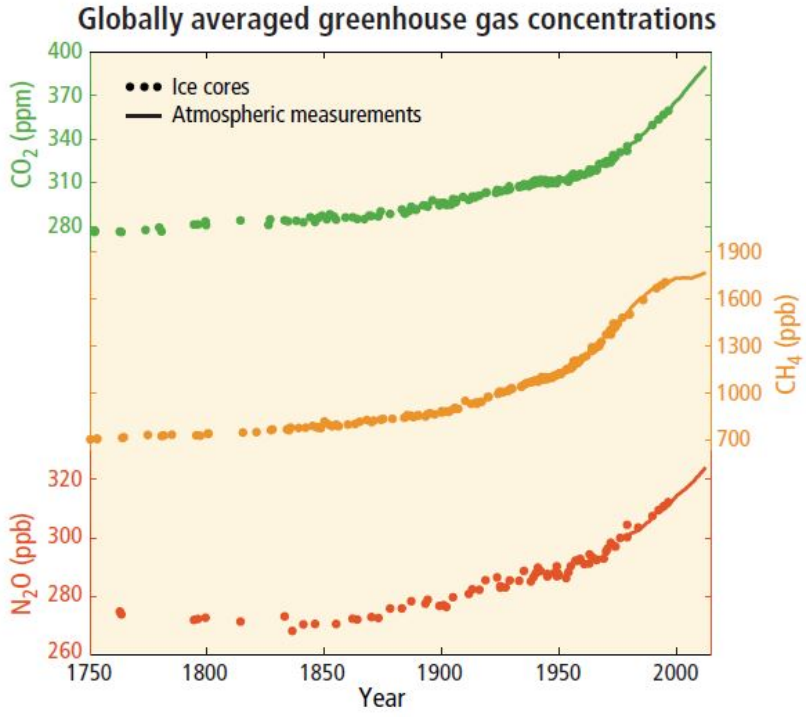

Figure 1.1 Observed changes in greenhouse gas concentrations [2]

Half of the anthropogenic CO_2 emissions during the Industrial Era have occurred in the last 50 years. Between 1970 and 2010 CO_2 emissions from fossil fuel combustion and industrial processes contributed about 78% to the total greenhouse gases emission increase (see Figure 1.2).

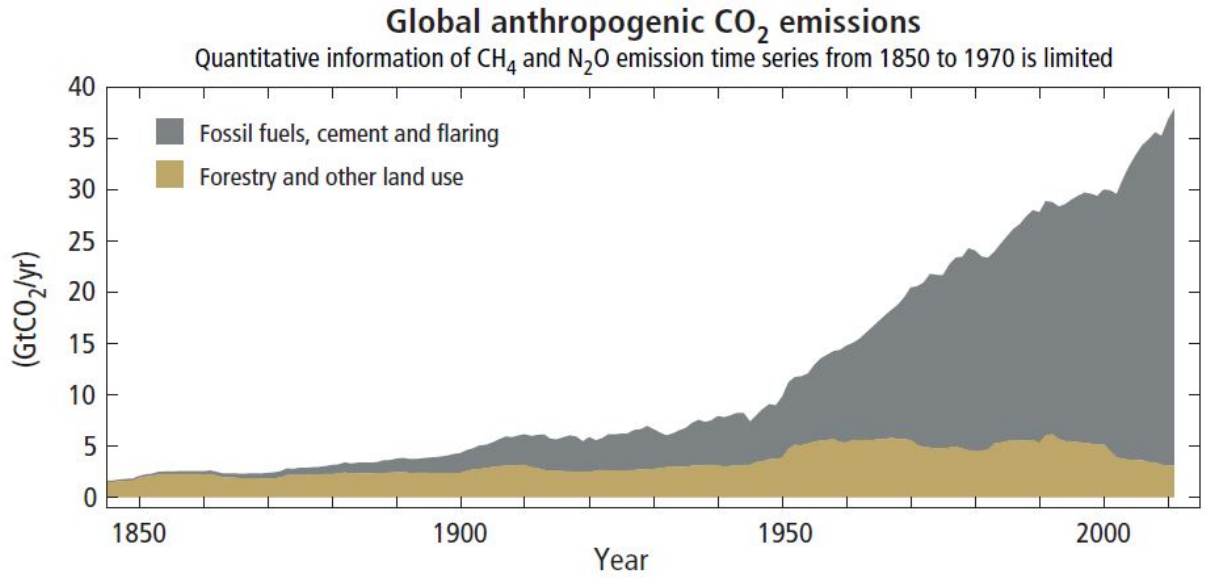

Figure 1.2 Annual global anthropogenic carbon dioxide (CO_2) emissions from fossil fuel combustion, cement production, flaring, forestry and other land use[2].

The Mediterranean climate is characterized by dry summers and mild, wet winters. It is a region particularly sensitive to climate changes due to its semi-arid conditions, its intermediate position between the high-latitude and subtropical atmospheric systems, its hydrological characteristics and its high climatic heterogeneity characterized by altitude gradients, microclimates and extreme seasonality [3], [4].

Atmospheric modes of variability, such as the Arctic Oscillation/North Atlantic Oscillation (AO/NAO), the East Atlantic (EA), the East Atlantic/Western Russian (EA/WR) patterns and the El Nino Southern Oscillation (ENSO) play an important role in seasonal temperature and precipitation variability, as well as in surface water heat fluxes that in turn have influence on the Mediterranean thermohaline circulation [5]–[12]. The Mediterranean is considered as a climatic hot spot where most countries are experiencing high frequency of droughts, water scarcity, forest fires, increasing desertification and rising air temperatures [2], [13]. These conditions are expected to be intensified in the future, having as a result deeper impacts on ecosystems and human societies [2], [14]. Consequently, extensive research has been conducted on both the study of future and past Mediterranean climates. Particularly, the Holocene period is of great interest since it involves the anthropogenic pressures on the environment.

Holocene is the geological period of approximately the last 11500 years that begins at the end of the last glacial period. The climate during this period has been fairly stable compared to the dramatic shifts of the last glacial cycle. These mild climate conditions gave the opportunity for the growth and development of modern society through the creation of stationary settlements, advanced agriculture and great flowering of the human culture. However, this period is characterized by centennial-millennial changes whose nature and chronological boundaries are not well-defined [15]. As for the Mediterranean region, evidence of complex spatial and temporal climatic variability with patterns from east to west and from north to south during the Holocene is provided by a large body of datasets [16]–[20]. Therefore, it is important to establish a denser network of proxy records around the Mediterranean that can contribute to our understanding of regional climatic differences within the basin and its various mechanisms as well as the relationship between the climate, the physical environment and human actions.

1.1 Mediterranean climate variability

The Mediterranean has experienced climatic, environmental and oceanographic changes in the past, often closely related to the northern hemisphere and the global scale variability [21], [22]. During the last two millennia there have been marked periods with climate changes in the Mediterranean that have been described in the literature [21]. These periods consist of: the Dark Ages Cold (DA) period from 300 to 600 AD with a marked drop in temperatures at 450 AD, the Medieval Climate Anomaly (MCA) period from 600 to 1200 AD characterized by warmer conditions, but interrupted by two cooler events at 700 and 1100 AD. Finally, there is the Little Ice Age (LIA) period from 1200 to 1850 AD, with cooling extremes occurring at around 1400 AD and 1625 AD.

According to Roberts *et al.* [18], the first six centuries AD cover some of the most excessive and long-lasting droughts of the late Holocene in the Middle Eastern region. In southern Greece this period is associated with a shift to several cold conditions of varying durations, strong variation in water availability and a generally more unstable climatic context [23]. During the 7th and 8th century AD, a phase of very high climatic instability has been identified [23]. High-resolution lake, marine and tree rings records from Iberia and Morocco suggest lower water levels and

higher salinities during the MCA and generally more humid conditions during the LIA [18], [24]. In contrast, lake and partly speleothem evidence from Turkey shows an opposite pattern of a wet MCA and a dry LIA for the Eastern Mediterranean [18]. Thus, an east-west climate seesaw pattern is proposed, which seems to take place during the last 1100 years between the eastern and western Mediterranean. However, whilst western Mediterranean aridity/humidity patterns appear consistent during the two periods, the pattern is less clear in the eastern Mediterranean region [18], [25], [26].

Several seasonal climate reconstructions have been presented for the last centuries that cover the eastern Mediterranean [25]–[31]. However, seasonal climatic information for the area is scattered and information about variability, trends and extremes at intraseasonal and interannual scale have therefore large uncertainties [21]. Notable fluctuations in seasonal temperatures are further affected by large tropical volcanic eruptions, e.g. the case of temperature drop during the Dalton solar minimum (ca 1790 to 1830 AD) [32].

1.2 Climate reconstructions

Instrumental records offer valuable information to determine the past climate changes. Northern Hemisphere instrumental data considering temperatures measurements date back to the mid-1850's and ocean data are largely constrained to the last 50 years [33]. However, time series of measured environmental parameters often cannot capture short-term processes, rare events and non-analogue situations, since most of the times they are temporally inhomogeneous and spatially too inconsistent [34], [35]. Therefore, instrumental records fail to embrace the complete picture of climatic variability [36].

The oceans cover more than 70% of the Earth's surface and are a very important source of paleoclimatic information. Proxy indicators, preserved in the marine sediments, offer a wealth of physical, chemical and biological properties that reflect the climatic and oceanographic environment and are valuable for the reconstruction of paleoclimatic and paleoceanographic evolution. Sediments are composed of both marine and terrigenous materials. The marine component includes the remains of planktonic and benthic organisms, which provide a record of past climate and oceanic circulation, in terms of sea surface temperature and salinity, dissolved

oxygen in deep water, nutrient or trace element concentrations, etc. [37][38]. On the other hand, terrigenous material can provide a pattern of the continents' humidity-aridity variations, the intensity and direction of winds blowing from the land to the oceans, and other processes of sediment transport to the oceans. Marine sediments also contain organic molecules derived from terrestrial or marine organisms, called biomarkers, which can be useful proxies of paleoceanographic conditions or of paleoenvironmental conditions [39]–[41].

1.2.1 Biomarkers

Biomarkers are complex organic compounds that typically consist of carbon, hydrogen atoms, and other elements, which contribute to the organic matter, found in the marine and terrestrial environment and can be attributed to formerly living organisms. These molecules are preserved in sediments, rocks and crude oil [41]–[43]. Lipid biomarkers in the marine environment can be initially produced by organisms from the aquatic (e.g. alkenones produced by haptophytes) or the terrestrial environment (e.g. long chain *n*-alkanes derived from plant-waxes of higher plants).

Lipid biomarkers' importance relies upon their resistance against early degradation processes during transport, sedimentation and after burial into the sediments [39]. The most valuable biomarkers can be related to a certain group of organisms, and carry a signal from the environment in which they were synthesized. Lipid biomarker structures, abundances, ratios, and their stable isotope compositions provide valuable information on present and past environments. Thus, several lipid biomarker (quantitative and qualitative) proxies have been developed in paleoceanography aiming at reconstructing past sea surface temperatures (SSTs), sea surface salinity (SSS), marine primary and secondary productivity, upwelling intensity, soil inputs, changes in land vegetation and precipitation patterns etc. [40].

1.2.1.1 Long-chain *n*-alkanes and *n*-alkanols

Homologues of long chain *n*-alkanes and *n*-alkanols are typically found in terrestrial and marine sediments [44]–[49]. They are the major components of protective epicuticular waxes on the leaf

surfaces of higher land plants [42] and are relatively resistant to degradation [50]. They are transferred for long distances by winds or are delivered directly by rivers [40].

Plant-wax derived *n*-alkanes have a typical carbon chain-length between C_{25} and C_{35} and show a strong predominance of odd-carbon homologues over even-carbon homologues with the most dominant representatives being the C_{27}, C_{29}, C_{31} and C_{33} [42]. The magnitude of this odd-over-even predominance, expressed by the Carbon Preference Index (CPI) [51], is used to distinguish between plant (CPI>4 in plants) [52] and fossil fuel products (CPI~1) [53]. Chain length variations (average chain length-ACL) in land plant biomarker are commonly related to changes in the temperature and humidity/aridity in the growing environment of source vegetation, since plants tend to synthesize longer chain length waxy components in response to elevated temperatures [54]. Thus, changes in the vegetation cover during different climatic periods could be inferred by changes in the average chain length of terrestrial *n*-alkanes [55].

1.2.1.2 Long-chain alkenones

Long-chain alkenones reflect the productivity from algal species of the Prymnesiophyte class, e.g., Emiliania huxleyii [56], while, in general, the known biological precursors of long-chain diols are marine nannoplankton of the class Eustigmatophyta, and C_{30} keto-ols might be derived by oxidation of the corresponding C_{30} diols [57]. However, long-chain diols have also been identified in Proboscia diatoms [58][59]. Loliolides (isololiolide and loliolide) share several structural features characteristic of carotenoids in marine algae, which were proposed to serve as their biogenic precursors [60]. Marine sterols are major constituents of several marine phytoplankton groups such as prymnesiophytes, diatoms and dinoflagellates [61][62].

The $U^{k'}_{37}$ index is a very useful lipid-derived SST proxy and is based on long chain di- and tri-unsaturated alkenones with 37 carbon atoms. These alkenones are produced by a limited species of haptophyte algae e.g., *Emiliania huxleyi* and *Gephryocapsa oceanica* [56], [63]–[65], which inhabit the euphotic zone of the ocean. The $U^{k'}_{37}$ index is defined as the ratio of the di-unsaturated alkenone ($C_{37:2}$) relative to the sum of di- and tri-unsaturated alkenones ($C_{37:3}$). In cultures, field measurements and sediments, it is observed that the relative proportion of $C_{37:3}$ increases with decreasing ambient temperature [66], [67]. Global surveys on core tops confirmed

this relationship resulting in the development of calibration functions of $U^{k'}_{37}$ to mean annual SSTs [68], [69]. Regional calibrations try to account for deviations from this relation, which have been attributed to differences in depth of maximum alkenone production [52], [70]–[73] or seasonal blooming of haptophytes [71], [74]–[77]. Further discrepancies between $U^{k'}_{37}$ and SSTs may be introduced by selective degradation of $C_{37:3}$, resulting in warmer SST estimates [78]–[83]. Nonetheless, the $U^{k'}_{37}$ paleothermometer has been successfully applied for millennial scale SST reconstructions since the Late Pleistocene, in high-resolution studies covering the Holocene, and in combination with other SST proxies [84].

1.2.1.3 Steroid alcohols

Steroid alcohols (sterols), such as cholesterol ($27\Delta^5$), are essential lipids in eukaryotic membrane controlling the membrane permeability and rigidity [57]. An extensive variety of functionalized steroids was identified in recent sediments and is categorized by the number and position of double bonds, hydroxy-, oxo-, and alkyl groups, and other, often, complex, substituents. They can be diagnostic for a wide range of taxonomic groups, particularly algae [85]. However, during diagenetic degradation processes most of the functionalities are lost, leaving a limited number of sterols to be used as proxies [86].

1.2.1.4 Polycyclic Aromatic Hydrocarbons (PAHs)

Polycyclic aromatic hydrocarbons (PAHs) are ubiquitous in the environment. They constitute an important class of persistent organic pollutants. Some of them are known to have toxic, mutagenic and/or carcinogenic properties [87] and 16 among them are classified as priority pollutants by international environmental agencies (EEA-EU, EPA-US).

PAHs enter the marine environment through the atmosphere (dry/wet deposition, gas exchange across the air–water interface) but also through direct discharges, such as oil spills or industrial outfalls, oil seepage, continental run-offs and rivers [88]–[92]. PAHs are generally insoluble in water, so in the marine environment they tend to be adhered to particulate matter that is

suspended in the water. Hence, they are discarded from surface waters and transported to deep ocean waters [93]–[97].

1.3 Scope of the present thesis and structure

The main objective of the present thesis is to investigate the land-sea interactions in the Elefsis Bay during the last 300 years via the use of a plethora of marine and terrestrially-derived biogeochemical indices. Besides, by assessing these indices it is possible to gain a better understanding of the sensitivities and response modes of the study area to oceanographic, environmental and hydrological changes, as also as changes in the supply of terrestrial organic matter from the surrounding land to the core site, both of biogenic and anthropogenic origin. Furthermore, the results of this study could contribute to a denser network of coastal Eastern Mediterranean climate data.

Chapter 2 describes the study area and the multi-core location and age-depth model. In Chapter 3, the methodology and analytical protocol are presented. Chapter 4 introduces the results from the various biogeochemical indices retrieved from the WF-S2 sedimentary record. Chapter 5 focuses on the identification of land-sea interactions through the discussion on the biomarkers' trends. Finally in chapter 6, the concluding remarks are pointed out, while some suggestions for future research are proposed.

2 STUDY AREA

2.1 Saronikos Gulf

The Saronikos Gulf is situated at the West-Central Aegean Sea (northeast Mediterranean Sea). It communicates with the Aegean Sea to the east and is surrounded by the peninsulas of Attica to the north and Peloponnese to the southwest (Figure 2.1). There are several islands and islets in the gulf, Salamina and Aigina being the most important in terms of size and population density. The length of the coastline is ~ 270 km, the surface ~ 2.866 km^2 and the mean water depth ~ 100 m.

Figure 2.1 Saronikos Gulf and Elefsis Bay, located next to Athens

The circulation of the Saronikos Gulf has a distinct two-layer structure in the period from late spring to summer to late fall, whereas it is basically barotropic during the rest of the year from December to March [98].

Inner Saronikos Gulf, located at the northern part of the eastern basin, is exposed to intense anthropogenic pressure from several point and nonpoint pollution sources, as it constitutes the catchment area of the metropolitan city of Athens with approximately 4 million habitats [99][100]. Therein, numerous anthropogenic activities take place, such as industries, oil refineries, ship yards, marinas, touristic facilities e.t.c. especially at the industrial zone of Elefsis Bay and Piraeus port [101]–[103]. Besides, the Inner Saronikos receives the treated wastewaters of the aforementioned cities as well as of smaller surrounding towns from a point source (outfall) south of the Psittalia Island [104]. Most activities have direct input to the gulf's waters while others contaminate the soils or the groundwater affecting the marine environment via runoff and/or submarine groundwater discharges and the atmospheric deposition of pollutants from the adjacent urban areas. Moreover, amongst the most important nonpoint pollution sources of the Saronikos Gulf is the intense marine traffic resulting in substantial amounts of petroleum discharges. The later result in the presence of a chronic petroleum-associated anthropogenic background burden in sediments of the Inner Saronikos Gulf [102], [105]–[107].

2.2 Elefsis Bay

Elefsis bay is located at the Northern Saronikos Gulf in Greece next to the metropolitan area of Athens (Figure 2.1). It covers 67 km^2 with a maximum depth of 35 m (average depth 18 m) and is almost enclosed, except from two sills through which it communicates with the rest of Saronikos gulf. Estimates of the surface flow in Elefsis Bay showed a flow of around 250 $m^3 s^{-1}$ from east to west during winter and a higher (450 $m^3 s^{-1}$) reversed flow in summer [108],[109].

The Elefsis Bay has a different morphology compared to Saronikos Gulf. It has also suffered more from pollution during the last decades, mainly by industrial activities on its coastline. A significant number of industries (oil refineries, shipyards, chemical plants, food, metal cement industries etc.) are located along the northern coastline of the Bay. Extended water pollution caused by organic matter and metal enrichment from hot spots, casts a shadow over human

population growth and development. In the eastern reach of Elefsis Bay lies the city of Athens with a population of over three millions. The eastern Keratsini channel is enriched by the industrial and shipyard area of Piraeus harbor. Until 1994, Keratsini channel had been receiving the untreated domestic and industrial sewage of the Athens Metropolitan area which was discharged into the surface water layer of the channel and enriched the bay with metals, nutrients and organic matter. After 1994, the sewage of the Athens Metropolitan area was primarily treated in the Psitallia Sewage Treatment Plant and discharged into the inner Saronikos Gulf. Additionally, by the end of 2004, the secondary stage of the Psittalia Sewage Plant became operational.

The extended anthropogenic pollution of the area occurred after the Second World War, when rapid population growth and development followed with increasing industrialization. At that time, population growth, a large fertilizer factory situated just outside the entrance of Piraeus Harbor and the discharge of the untreated nutrient-rich sewage enhanced the point-source nutrient loading. After 1994, the pollution in the Bay decreased significantly, because many industries closed or decreased the amount of their pollutants according to the European and National directives. However, during the last years, there has been a turn towards cleaner technologies, and the bay does not receive the large amount of untreated sewage of Athens any longer[110]. At the same time, the bay does not receive any significant amounts of natural fresh waters either, since no river water flows into the bay, except for some ephemeral streams in winter.

The aforementioned anthropogenic inputs lead to ecological stress in the bay. Documented anoxic conditions in the deepest western part (>25 m depth) of the Bay date back to the summer of 1973 [111], when the zooplanktonic biomass remained near zero [112]. Following the initial documentation of anoxia, several low dissolved oxygen (DO) conditions have been referred [113][114][115][116][117][118]. Hypoxic and anoxic conditions are being developed every year only in the western part of the Elefsis Bay and they are leading to an enrichment of organic matter in the sediments. The dark to black color of the surface sediments is an index of the high content of organic matter in the sediments [119].

In short, the physical setting of the Elefsis Bay, the narrow and shallow connections to the Saronikos Gulf with low freshwater inflows and limited water exchange, leads to a strong

seasonal density stratification of the water mass and influences the oxygen distribution in the basin, resulting in hypoxia and anoxia, existing for about 5 months. The summer stratification reduces the supply of DO to the bottom layers, whereas, oxidation of the organic matter results in the disappearance of oxygen and the formation of anaerobic conditions. This situation retains nutrients and organic matter within the basin and leads to high nutrient accumulation [119].

Extensive research has been conducted during the last 50 years concerning the Elefsis Bay. Scoullos [120] suggests that the upper part of the sediment column is greatly enriched with lead of anthropogenic origin, which is mainly associated with fine particles. The metal pollution in the Elefsis Bay causes relatively medium levels of oxidative stress in tissues of mussels due to cellular oxy-radical generation [110]. Surface seawater and tissues samples of indigenous black mussels, *Mytilus galloprovincialis*, have been collected from three coastal sites of Saronikos Gulf and from the Elefsis Gulf. PAHs composition was dominated by two-, three- and four-ring compounds in seawater, where 17 different PAH compounds were identified and measured in mussel tissues [121]. Studies reveal that after the start of the operation of Psitallia Wastewater Treatment Plant, the levels of trace metal pollution of the marine environment of the gulf are possibly reaching a steady state [122].

2.3 Core location and chronology

The multicore WF-S2 was retrieved by the R/V AEGAEO (HCMR) in 2014 from the deepest part of the Elefsis Bay (longitude: 23.450; latitude: 38.007) as shown in Figure 2.2. The 52-cm long core was sampled continuously at a sampling step of 0.5 cm.

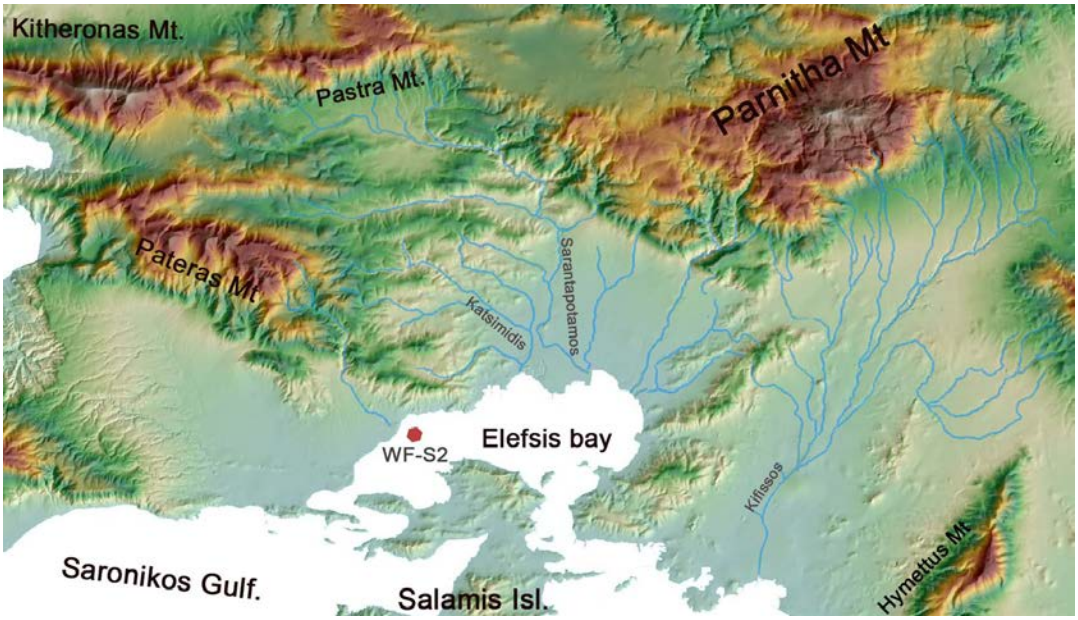

Figure 2.2 The multicore WF-S2 was retrieved from the deepest part of the Elefsis Bay

The age-depth model of the core was constructed using the software Bacon 2.2, two accelerator mass spectrometry (AMS) ^{14}C datings with a marine reservoir effect (ΔR) value of 73 (±60) ^{14}C years and the beginning of the Industrial Period (1880 AD), recognized by the increase of UCM at 18cm depth. The sequence is a continuous, high resolution palaeoenvironmental archive of the last 300 years with its base dating back to 1660 AD (± 90).

Table 2-1 Accelerator mass spectrometry (AMS) ^{14}C datings.

Depth (cm)	^{14}C measured age (years BP)	Calibrated age (years BP)	Material
35	540 ± 30	170 – 210	Marine molluscs
50 - 52	680 ± 30	300 - 360	Planktonic forams

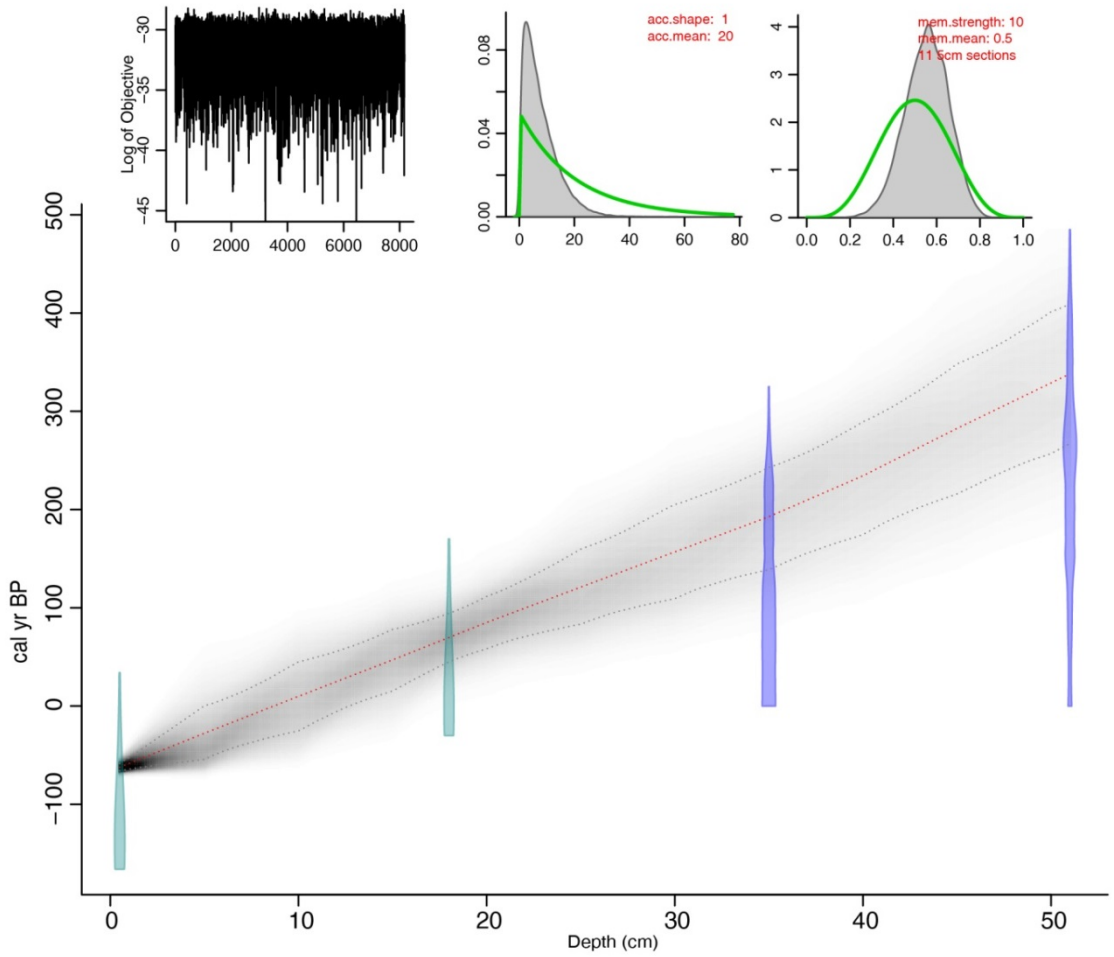

Figure 2.3 Age model for the WF-S2 core, using Bacon 2.2, and the reference datings.

3 METHODOLOGY

3.1 Materials

One of the major problems in compounds analysis is contamination. This is even more important in the case of low concentration samples like environmental samples. Contamination may arise from the collection of the samples, their transfer to the lab or from the various analytical steps. It is essential to have very clean materials and to choose solvents of high purity. All solvents and silica gel (230–400 mesh) were purchased from Merck ('Suprasolv', Darmstadt, Germany). Standard compounds were obtained from Sigma-Aldrich (MO, USA) and Dr. Ehrenstorfer GmbH.

Silica gel was soxhlet extracted with dichloromathane overnight and kept dry (in desiccator) until use. All glassware was combusted at 450^{o}C prior to use.

The analysis of blank samples in parallel to the environmental samples is of great importance so as to ensure that the results are correct. From the analysis of our blank samples the contamination was below the detection levels.

3.2 Organic carbon and stable isotopic analysis

Fifty one samples were collected at a resolution step of 1 cm for the determination of total carbon (TC), total nitrogen (TN), organic carbon (OC) contents and stable isotopic composition of OC ($\delta^{13}C$) and nitrogen ($\delta^{15}N$). The analysis was carried out at the University of California, Davis. The freeze-dried and ground sediments were initially de-carbonated using repetitive additions of a 25% HCl (*v/v*) solution, separated by 60^{o}C drying steps, until no effervescence was observed [123]. The analysis was carried out using a Flash 1112 EA elemental analyzer interfaced to a Delta C Finnigan MAT isotope ratio mass spectrometer. Stable carbon and nitrogen isotope ratios are expressed as $\delta^{13}C$ and $\delta^{15}N$ values against V-PDB (Pee Dee Belemnite standard) for carbon and atmospheric N_2 for nitrogen. The overall analytical error based on duplicate measurements was ±0.2 ‰ for $\delta^{13}C$ values and ±0.3 ‰ for $\delta^{15}N$ values.

3.3 Lipid extraction and separation

The analytical protocol of Gogou et al. (1996) [124], was slightly modified and used for the qualitative and quantitative determination of lipid biomarkers in the considered sediment samples.

Prior to the analytical procedure (see Figure 3.1), the sediments were freeze-dried and after that a mortar was used to grind them into a fine powder and thus homogenize the sample. From the homogenized sample 1-5 g were used for the extraction, depending on the total organic carbon concentration.

Regarding the analytical procedure, the samples were initially spiked with a mix of internal standards for quantitative determinations. The internal standards used were:

- 10μL of a mix of perdeuterated internal standards of hydrocarbons (9.64 ppm of [$^2H_{50}$]*n*-tetracosane for aliphatic hydrocarbons; [$^2H_8$]napthalene, [$^2H_{10}$]acenaphthene, [$^2H_{10}$]phenanthrene, [$^2H_{12}$]pyrene, [$^2H_{12}$]chrysene, [$^2H_{12}$]perylene and [$^2H_{12}$]benzo[*ghi*]perylene for PAHs-10 ppm)
- 25μL of *n*-$C_{21}D_{43}O$ (25.4 ppm)/5α-androstan-3β-ol (25.8 ppm)
- 25μL (21.92 ppm) of *n*-$C_{36}H_{74}$ (surrogate standard for the fraction containing the long chain alkenones)

The organic compounds were extracted from the freeze-dried sediments with a mixture of dichloromethane /methanol (4:1 *v/v*) by sonication. The extraction scheme was repeated three times. After that the extracts were transferred to a clean pear-shaped glass flask through infiltration using glass wool and Na_2SO_4 as a desiccant. The total extract was concentrated in a rotary evaporator, transferred to a 1-mL amber glass vial, and further evaporated under a gentle nitrogen stream. In the highly polluted samples (upper part of the core), prior to evaporation, sulfur was removed over a few hours using copper wires.

Then the extract was fractionated into individual compounds classes by column chromatography on silica gel.

For every column, 0.45 g of silica gel was used, which was previously activated for 1 h at 150^{o}C. The following solvent systems with increasing polarity were used to elute the different compound classes:

1. F1 fraction (aliphatics): *n*-hexane
2. PAHs fraction: toluene/*n*-hexane (1:9)
3. F2 fraction (carbonyl compounds such as long chain alkenones): dichloromethane/n-hexane (2:3)
4. F3 fraction (*n*-alkanols and steroidal alcohols): ethyl acetate/*n*-hexane (1:2)

The method used to prepare the column is the dry method. The base of the glass column contains a glass wool plug to hold the solid phase in place. The column is prepared by packing the solid absorbent (silica gel) on top of the glass wool. Silica gel acts as the stationary phase and is followed by the mobile phase, which is flushed through the column until it is completely wet, and from this point on is never allowed to run dry [125]. The sample is placed carefully into the top of the column using a pipette. A clean pear-shaped glass flask is placed under the column in order to collect the eluate. For each fraction a different glass flask is used. The eluate is evaporated in a rotary evaporator and transferred to a 1-mL conical vial under a gentle nitrogen stream.

3.4 *n*-Alkanols and steroidal alcohols derivatization

n-Alkanols and steroidal alcohols were derivatized to the corresponding trimethylsilyl ethers prior to GC-MS analysis, as follows: the fraction containing the *n*-alkanols and steroidal alcohols was initially evaporated in a rotary evaporator until about 1 mL volume, and then under a gentle stream of nitrogen to dryness. 100 μL of N,O-bis-(trimethylsilyl)-trifluoroacetamide (BSTFA) were added; the reaction mixture was shaken vigorously and allowed to stand for 1 h at 90 ^{o}C. After that, the reaction mixture was evaporated under a nitrogen stream to dryness. Finally, isooctane was added till the volume of 50 μL, so that the chromatographic analysis could be carried on.

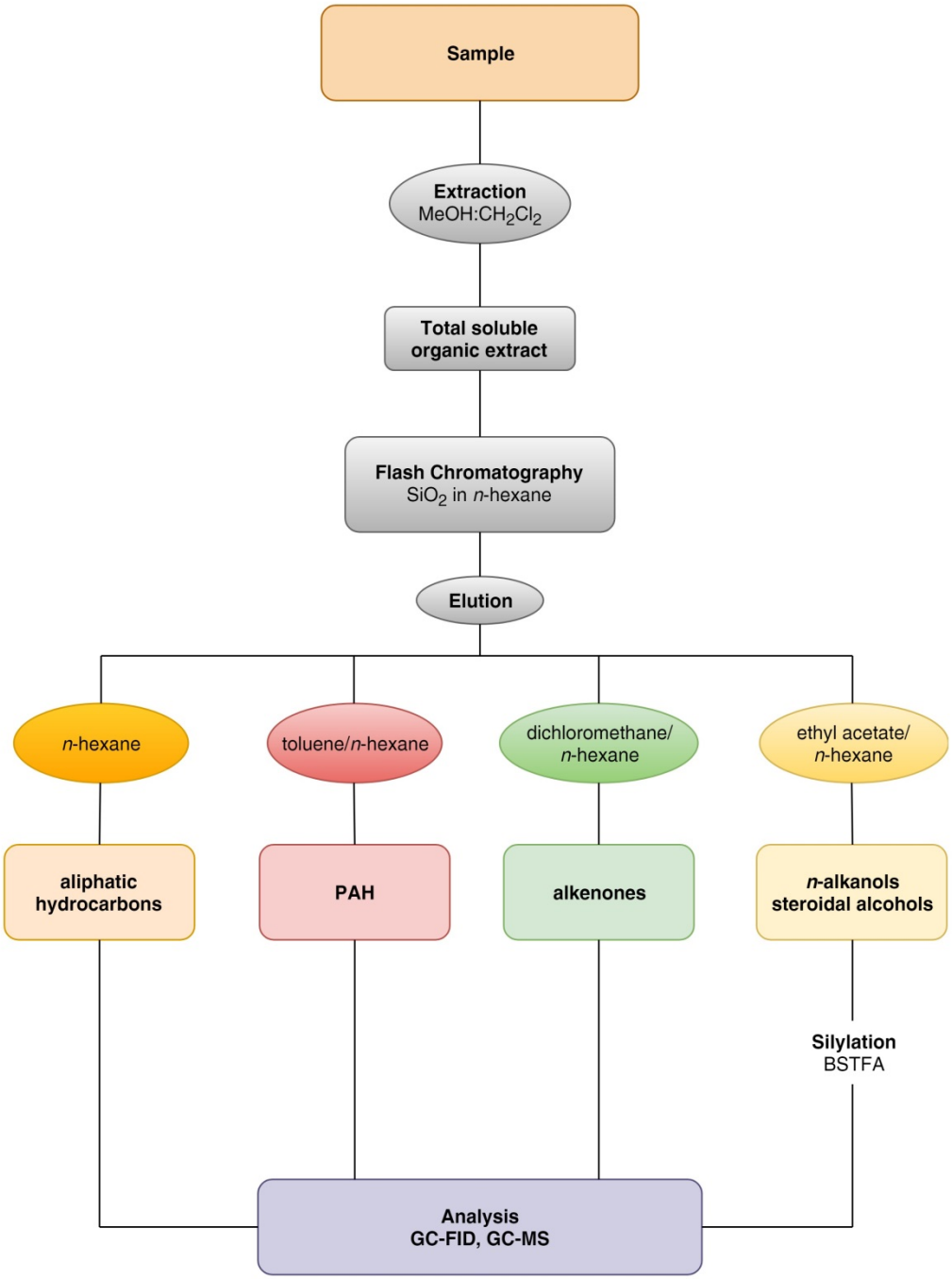

Figure 3.1 Scheme of the entire analytical procedure

3.5 Identification and quantitative determination (GC-FID and GC-MS)

The considered organic compound classes usually exist in low concentrations in environmental samples. So there is a need for high precision and analytical power techniques.

The instrumental analysis was carried out by gas chromatography mass spectrometry (GC-MS) on an Agilent 7890 GC, equipped with an HP-5MS capillary column (30m×0.25mm i.d. × 0.25 μm phase film), coupled to an Agilent 5975C MSD. For the analysis of aliphatic hydrocarbons and sterols/*n*-alkanols the MSD operated in full scan mode and the GC oven temperature was initially held at 60 ^{o}C for 2 min, brought to 80 ^{o}C at a rate of 25 ^{o}C min^{-1}, then to 300 ^{o}C at a rate of 5 ^{o}C min^{-1} (3 ^{o}C min^{-1} in the case of sterols/*n*-alkanols) and finally held at 300 ^{o}C for 35 min. PAHs were analyzed using a selected ion monitoring (SIM) acquisition program. The oven temperature program was the same as in the case of aliphatic hydrocarbons but with a 300 ^{o}C final isothermal of 6 min. Helium (99.999% purity) was used as carrier gas at a flow of 1.1 mL min^{-1}. As far as the long chain alkenones is concerned, the compound identification was performed by GC-FID. The GC-FID analyses were carried out on a Hewlett Packard gas chromatograph, model 5890 with Hewlett Packard Chemstation data system, fitted with an on-column injector, and a fused silica capillary column (HP-5, 50 m × 0.17 μm × 0.32 mm). Helium (99.999% purity) was used as carrier gas at a flow of 1.1 mL min^{-1}. The chromatographic conditions were the following: detector temperature 300 ^{o}C; temperature program: 50 ^{o}C (1 min); 50–220 ^{o}C (25 ^{o}C min^{-1}), 220–300 ^{o}C (5 ^{o}C min^{-1}), and 300 ^{o}C (30 min).

The aliphatic fraction consists of the *n*-alkanes and the UCM. As far as the *n*-alkanes is concerned, the homologues from *n*-C_{24} to *n*-C_{35} were identified. Besides, the long-chain alkenones with 37 and 38 carbon atoms and the n-alkanols from *n*-C_{14} to *n*-C_{32} were determined. Also alkanediols-1,15 (diols), keto-15-alkanols-1 (keto-ols) C_{30}, and C_{32} and isololiolide and loliolide were identified. Finally, a wide range of steroid alcohols (Table 3-2) and PAHs (Table 3-3) were determined.

The signal of the unresolved complex mixture (UCM) of aliphatic hydrocarbons was defined by the chromatographic area (fraction F1) between the solvent baseline and the curve defining the base of resolved peaks. UCM quantification was performed relatively to [2H50] *n*-tetracosane using the average response factor of *n*-alkanes[126].

The individual lipid components were identified by a combination of comparison of GC-retention times to authentic standards and comparison of their mass-spectral data to those in the literature. Quantification was based on the GC-FID or GC-MS response and achieved by comparison of peak areas with those of internal standards.

Standard solutions of the targeted PAH compounds, purchased from Dr. Ehrenstorfer GmbH, were spiked with the internal standards and run on each injection set in order to derive relative response factors (RRFs) of the analytes.

3.6 Lipid biomarkers and their application

The detailed study of a variety of lipid biomarkers in paleoceanographic studies permits to both autochthonous and allochthonous sources contributing to the sedimentary organic matter, delivering information on marine and terrestrial ecosystem responses to anthropogenic pressure and land-ocean interactions [127][128][124][129][130].

Considering that the organic carbon (OC) can vary due to the supply of inorganic material [127], the lipid biomarkers that were calculated were also normalized to the OC contents.

3.6.1 *n*-Alkanes and *n*-alkanols

Aliphatic hydrocarbons derive from natural sources such as terrestrial plant waxes, marine phytoplankton and bacteria [131], while they are also major components of petroleum products [53]. High molecular weight *n*-alkanes and *n*-alkanols are major components of epicuticular higher plant waxes [42][40] and have been often used as proxies of allochthonous natural (terrestrial) inputs from leaf waxes of higher plants [52][124]. The sum of the concentrations of the most abundant high molecular weight *n*-alkanes and *n*-alkanols of terrestrial origin are defined, respectively, as:

$$Ter_{NA} = n - C_{27} + n - C_{29} + n - C_{31} + n - C_{33} \quad (1)$$

and

$$Ter_{NA-OH} = n - C_{24-OH} + n - C_{26-OH} + n - C_{28-OH} + n - C_{30-OH} \quad (2)$$

The values measured for the *n*-alkanes are biased by the occurrence of petroleum hydrocarbons. Thus, two vertical profiles have been constructed for the *n*-alkanes. The one, referred to as "bias", includes the contribution of petroleum hydrocarbons. The other, referred to as "non bias", was calculated by subtracting the average of the next higher and lower even carbon numbered homologue[132], [133], as:

$$n - C_n = [C_n] - 0.5[\, C_{n+1} + C_{n-1}] \quad (3)$$

The Carbon Preference Indices of long chain *n*-alkanes (CPI_{NA}) and *n*-alkanols ($CPI_{N\text{-}OH}$) have been used as indicators of terrestrial organic matter degradation with CPI values in fresh leaves being typically >4 [52], although the occurrence of petroleum hydrocarbons bias (lower) CPI_{NA} values with increasing petroleum contribution, since fossil fuel products present CPI_{NA} values ~1 [53]. The indices were calculated, respectively, as:

$$CPI_{NA} = \frac{n - C_{25} + n - C_{27} + n - C_{29} + n - C_{31} + n - C_{33}}{n - C_{24} + n - C_{26} + n - C_{28} + n - C_{30} + n - C_{32}} \quad (4)$$

and

$$CPI_{N-OH} = \frac{n - C_{24-OH} + n - C_{26-OH} + n - C_{28-OH} + n - C_{30-OH} + n - C_{32-OH}}{n - C_{23-OH} + n - C_{25-OH} + n - C_{27-OH} + n - C_{29-OH} + n - C_{31-OH}} \quad (5)$$

Chain length variations in land plant biomarkers are commonly related to changes in the temperature and humidity/aridity in the growing environment of source vegetation, since plants tend to synthesize longer chain length waxy components in response to elevated temperatures

[54]. Thus, changes in the vegetation cover during different climatic periods could be inferred by changes in the average chain length of terrestrial n-alkanes [55]:

$$ACL = \frac{27 \times n-C_{27} + 29 \times n-C_{29} + 31 \times n-C_{31} + 33 \times n-C_{33}}{n-C_{27} + n-C_{29} + n-C_{31} + n-C_{33}} \quad (6)$$

Unresolved complex mixture of aliphatic hydrocarbons

The unresolved complex mixture (UCM) of aliphatic hydrocarbons, a commonly observed contaminant mixture in marine sediments consisting of branched alicyclic hydrocarbons [134], has been proven as toxic to sediment-dwelling organisms [135][136]. As far as the study area is concerned, UCM originates from chronic-oil pollution and/or coal combustion.

3.6.2 Isoprenoid derivatives

Loliolide (1,3-dihydroxy-3,5,5-trimethylcyclohexylidene-4-acetic acid lactone) is a monoterpene. The origin of loliolide has been discussed by several authors, and they suggested that loliolide is a degradation [137] or a photo-oxidation product of algal carotenoids such as fucoxanthin and zeaxanthin [138], [139]. As such, loliolide is used as a biomarker for photo-oxidative alterations of phytoplankton in sediments [140]. Loliolides (isololiolide and loliolide) share several structural features characteristic of carotenoids in marine algae, which were proposed to serve as their biogenic precursors [60].

3.6.3 *n*-Alkan-1,15-diols and keto-ols

The known biological precursors of long-chain diols are marine nannoplankton of the class Eustigmatophyta and C_{30} keto-ols might be deriving by oxidation of the corresponding C_{30} diols [57]. However, long-chain diols have also been identified in Proboscia diatoms [58][59].

3.6.4 Long-chain alkenones

Long-chain alkenones reflect the productivity from algal species of the Prymnesiophyte class, e.g., *Emiliania huxleyii* [56].

The ratios of the concentrations of long-chain alkenone homologues that differ in the degree of unsaturation might be used in the assessment of palaeo- sea surface temperature through the use of $U^{k'}_{37}$ index[67], [68], [72], [141]:

$$U_{37}^{k'} = \frac{C_{37:2}}{C_{37:2} + C_{37:3}} \tag{7}$$

and the global calibrated parameters of Conte et al.[69] :

$$T = -0.957 + 54.293 \times \left(U_{37}^{k'}\right) - 52.894 \times \left(U_{37}^{k'}\right)^2 + 28.321 \times \left(U_{37}^{k'}\right)^3 \tag{8}$$

There is an uncertainty associated with the alkenone to SST calibration that, according to Conte et al.[69] is >1 ^{o}C at the 68% confidence level. These values do not represent the full uncertainty associated with the reconstruction and it is worth to note that a quantitative estimation of the uncertainties cannot be achieved within the implemented modeling framework.

In the Aegean Sea, coccosphere fluxes indicate that the main alkenone producer *Emiliania huxleyii* is the dominant species all year round, with higher production and export rates occurring between March and June and secondary maximum from June to November [142][143]. Therefore, the estimated alkenone patterns and consequently the reconstructed alkenone SSTs are considered to reflect mean annual temperature values.

In Table 3-1 the calculated long-chain alkenones are presented:

Table 3-1 Long-chain alkenones identified in the WF-S2 core.

$C_{37:3}$	tri-unsaturated C_{37} ketone
$C_{37:2}$	di-unsaturated C_{37} ketone
$C_{38:3}$ et	tri-unsaturated C_{38} ethyl ketone

$C_{38:3}$ me	tri-unsaturated C_{38} methyl ketone
$C_{38:2}$ et	di-unsaturated C_{38} ethyl ketone
$C_{38:2}$ me	di-unsaturated C_{38} methyl ketone

3.6.5 Steroid alcohols

Steroid alcohols are essential lipids in eukaryotic membrane controlling the membrane permeability and rigidity [57]. An extensive variety of functionalized steroids was identified in recent sediments and is categorized by the number and position of double bonds, hydroxy-, oxo-, and alkyl groups, and other, often, complex, substituents. They can be diagnostic for a wide range of taxonomic groups, particularly algae [85]. Marine sterols are major constituents of several marine phytoplankton groups[61][62]. Those employed as marine biomarkers in this study consist of brassicasterol and dinosterol. Brassicasterol ($_{28}\Delta^{5,22E}$) is the major sterol in many diatoms but it also occurs in some prymnesiophytes, mainly Emiliania huxleyi, while dinosterol ($_{30}\Delta^{22E}$) is a major compound in dinoflagellates and is commonly used as source-specific biomarkers of this algal specie [57], [61]. The systematic names and the abbreviations (containing structural information: number/position of double bonds) of sterols detected in WF-S2 core sediments are depicted in Table 3-2.

Table 3-2 Nomenclature of the steroidal alcohols in the WF-S2 core. Annotated with (*) are those that were not identified in the core.

	Abbreviation	**IUPAC nomenclature**	**Other name**
S1	$26\Delta^{5,22E}$	24-norcholesta-5,22(E)-dien-3β-ol	
S2	$26\Delta^{22(E)}$	24-nor-5α(H)-cholest-22(E)-en-3β-ol	
S3		5β(H)-cholestan-3β-ol	Coprostanol
S4		5β(H)-cholesta-3α-ol	Epicoprostanol
S5	$27'\Delta^{5,22E}$	27-nor-24-methylcholesta-5,22(E)-dien-3β-ol	

S6	$27\Delta^{22E}$	27-nor-24-methyl-5*α*(H)cholest-22(E)-en-3*β*-ol	
S7	$27\Delta^{5,22E}$	cholest-5,22(E)-dien-3*β*-ol	Dehydro-22-cholesterol
S8		5*α*(H)-cholest-22(E)-en-3*β*-ol	
S9	$27\Delta^{5}$	Cholest-5-en-3*β*-ol	Cholesterol
S10	$27\Delta^{0}$	5*α*(H)-cholestan-3*β*-ol	Cholestanol
S11	$28\Delta^{5,22E}$	24-methylcholesta-5,22-dien-3*β*-ol	Brassicasterol
S12	$28\Delta^{22E}$	24-methyl-5*α*(H)-cholest-22(E)-en-3*β*-ol	Brassicastanol
*S13		24-methylenecholest-5-en-3*β*-ol	
S14	$28\Delta^{5}$	24-methylcholest-5-en-3*β*-ol	Campesterol
*S15		24-methyl-5*α*(H)-cholestan-3*β*-ol	
*S16		23,24-dimethycholesta-5,22(E)-dein-3*β*-ol	
S17	$29\Delta^{5,22E}$	24-ethylcholesta-5,22(E)-dien-3*β*-ol	Stigmasterol
S18	$29\Delta^{22}$	24-ethyl-5*α*-cholest-22-en-3*β*-ol	Stigmastanol
*S19		4*α*,24-dimethyl-5*α*(H)-cholest-22(E)-en-3*β*-ol	
*S20		23,24-dimethyl-cholest-5-en-3*β*-ol	
S21	$29\Delta^{5}$	24-ethylcholesta-5-en-3*β*-ol	Sitosterol
S22	$29\Delta^{0}$	24-ethyl-5*α*(H)-cholestan-3*β*-ol	Sitostanol
S23	$30\Delta^{22E}$	4*a*,23,24-trimethyl-5*α*(H)cholest-22(E)-en-3*β*-ol	Dinosterol
S24	$30\Delta^{0}$	4*a*,23,24-trimethyl-5*α*(H)cholestan-3*β*-ol	

The sum of concentrations of the considered lipid biomarkers of algal origin was calculated as follows:

$$\Sigma Algal = 28\Delta^{5,22E} + 30\Delta^{22E} + C_{30,diols\ \&\ keto-ols} + C_{37,alkenones} + loliolide + isololiolide \quad (9)$$

3.6.6 Polycyclic Aromatic Hydrocarbons (PAHs)

PAHs have their origin in anthropogenic activities such as biomass burning, incomplete combustion of fossil fuels and their byproducts, industrial processes and petroleum processing/transportation [144]. Some compounds such as retene and perylene may have natural sources [145], [146]. Both low and high molecular weight PAHs were determined in this study, as well as their methylated homologues. The names and the abbreviations (containing structural information: number/position of double bonds) of PAH detected in WF-S2 core sediments are given in Table 3-3.

Table 3-3 PAH compounds identified in the WF-S2 core.

Compound	Abbreviation
Phenanthrene	Phe
Methyl-phenanthrene	C_1-Phe
Dimethyl-phenanthrene	C_2-Phe
Trimethyl-phenanthrene	C_3-Phe
Anthracene	Anth
Retene	Ret
Fluoranthene	Flth
Pyrene	Pyr
Methyl-pyrene	C_1-Pyr
Dimethyl-pyrene	C_2-Pyr
Benzo[a]anthracene	BaA
Chrysene/Triphenylene	Chry/Tri
Methyl-chrysene	C_1-Chry
Dimethyl-chrysene	C_2-Chry

Benzo[*b*]fluoranthene	BbF
Benzo[*k*]fluoranthene	BkF
Benzo[*b*,*j*,*k*]fluoranthenes	Bflths
Benzo[*e*]pyrene	BeP
Benzo[*a*]pyrene	BaP
Perylene	Per
Indeno[1,2,3-*c*,*d*]pyrene	IndP
Benzo[*g*,*h*,*i*]perylene	BgP
Dibenzo[*a*,*h*]anthracene	DBA

4 RESULTS

4.1 Sea surface temperatures

Alkenone-derived SSTs at Elefsis Bay vary at the range of 22^{o}C to 25.1^{o}C. The minimum value is traced back to around 1770 AD and the maximum to around 1910 AD. SSTs drop by almost 1^{o}C from the first quarter of the 17th to the beginning of the 18th century. After that and throughout the 18th century, SSTs stabilize at a mean temperature of 23^{o}C. During the 19th century a gradual increase of 1^{o}C is observed. After the last decades of the 19th century, the SST values increase in just three decades 1^{o}C more. The trend of the SST values shows a decrease of 1.2^{o}C during the 20th century (see Figure 4.1).

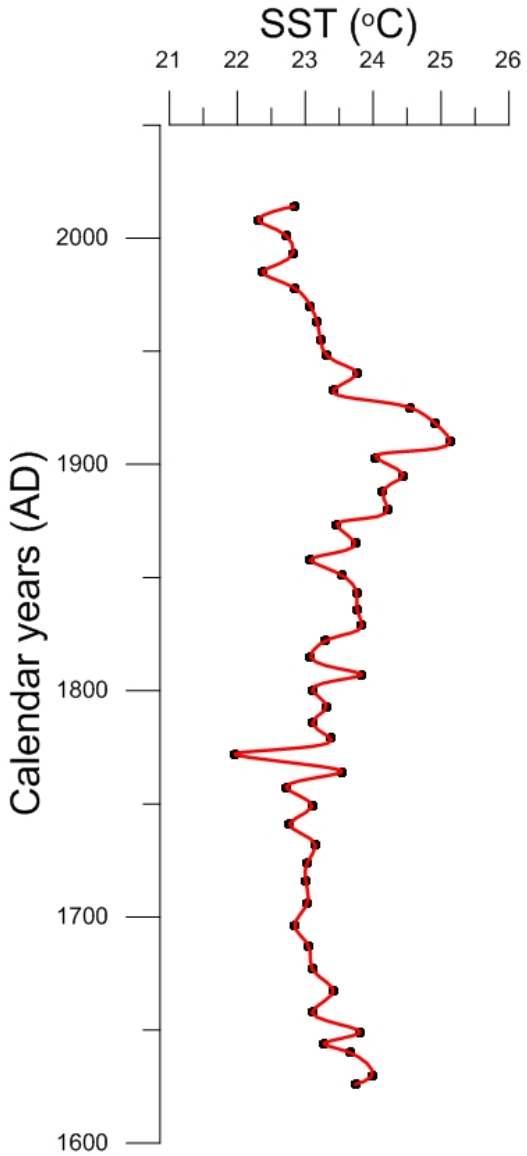

Figure 4.1 Sea Surface Temperatures (SST) calculated according to Conte et al. [69]

4.2 Total Organic Carbon (TOC), $\delta^{13}C_{org}$ and $\delta^{15}N$

The values of the organic carbon (OC) content in the examined sediment core ranged from 0.82 to 3.84%. Its vertical profile is shown in Figure 4.2, where it is obvious that it can be divided into two sections. The first section refers to the period from the bottom (around 1620 AD) of the core until the last decades of the 19th century. During this period OC values vary between 0.82 and 1.74% with a mean value of 1.17%. The second section refers to the period from the end of the 19th century till present day. The OC values within this section range from 2.82 to 3.84% and have a mean value of 3.48%.

Concerning $\delta^{13}C$, the minimum value is -20.07‰ at the beginning of the 21st century, while the maximum is -18.74‰ at the end of the 19th century. From the bottom of the core (around 1620 AD) until the first quarter of the 18th century a decreasing trend for $\delta^{13}C$ values is observed. After that and until the beginning of the 20th century the trend becomes increasing, particularly after the last decades of the 19th century. The last period (until today) turns back to a decreasing mode (see Figure 4.2).

The values of $\delta^{15}N$ in the studied sediment core vary in the range of 2.67 and 6.76‰. The vertical profile of $\delta^{15}N$ is presented in Figure 4.2. From the bottom of the core (around 1620 AD) until the last decades of the 19th century the values are slightly increasing with a mean value of 3.54‰. After that period there is a radical increase of the values. They range from 4.45 to 6.76‰ and the mean value is 5.57‰.

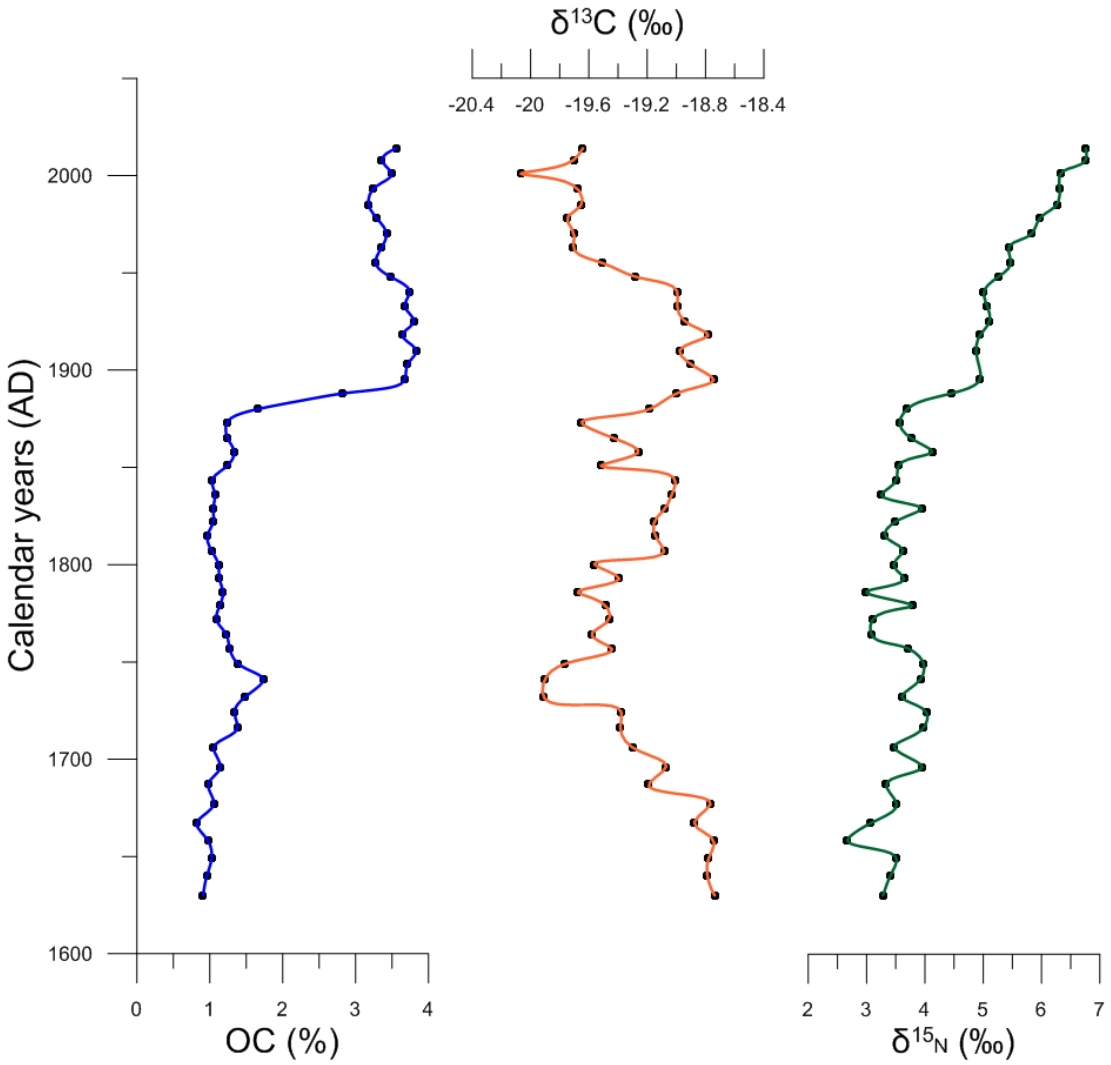

Figure 4.2 Total Organic Carbon (%), $\delta^{13}C$(‰) and $\delta^{15}N$(‰) vertical profiles in the studied sediment core

4.3 Lipid Biomarkers

4.3.1 Aliphatic hydrocarbons

The aliphatic hydrocarbons fraction is characterized by the presence of a series of *n*-alkanes ranging from *n*-C_{27} to *n*-C_{33} and a UCM. The distribution of the *n*-alkanes is dominated by odd-carbon-number homologues with maxima at *n*-C_{31}.

In Figure 4.3 the chromatogram for the bottom of WF-S2 core is depicted. The odd-carbon-number homologues are clearly dominating.

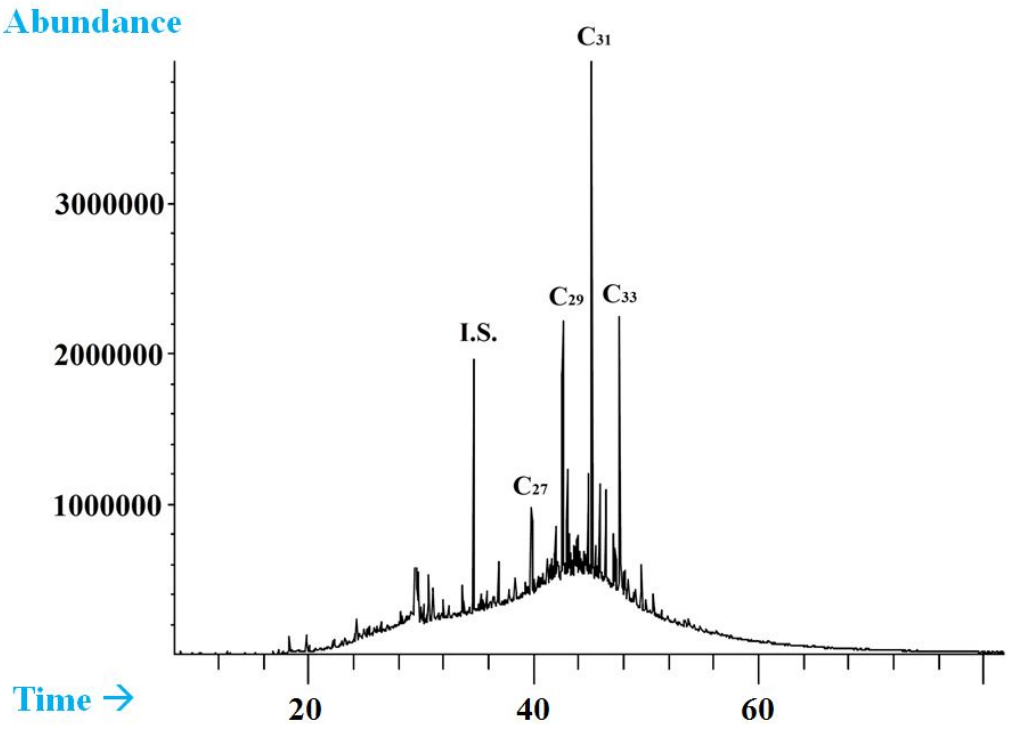

Figure 4.3 Characteristic chromatogram (full scan mode) of the bottom (49 cm depth) of the core

At the upper part of the core (Figure 4.5), the dominance of *n*-C31 homologue is still obvious. Besides, a series of C_{27}-C_{35} hopanes were identified (Figure 4.4), exhibiting a dominant thermodynamically stable 17α(H), 21β(H)- configuration, with 17β(H), 21α(H)- compounds being less prominent, while extended C_{31}-C_{35} homologues were present as pairs of the C_{22} diastereoisomers (22S and 22R). The UCM is very distinct.

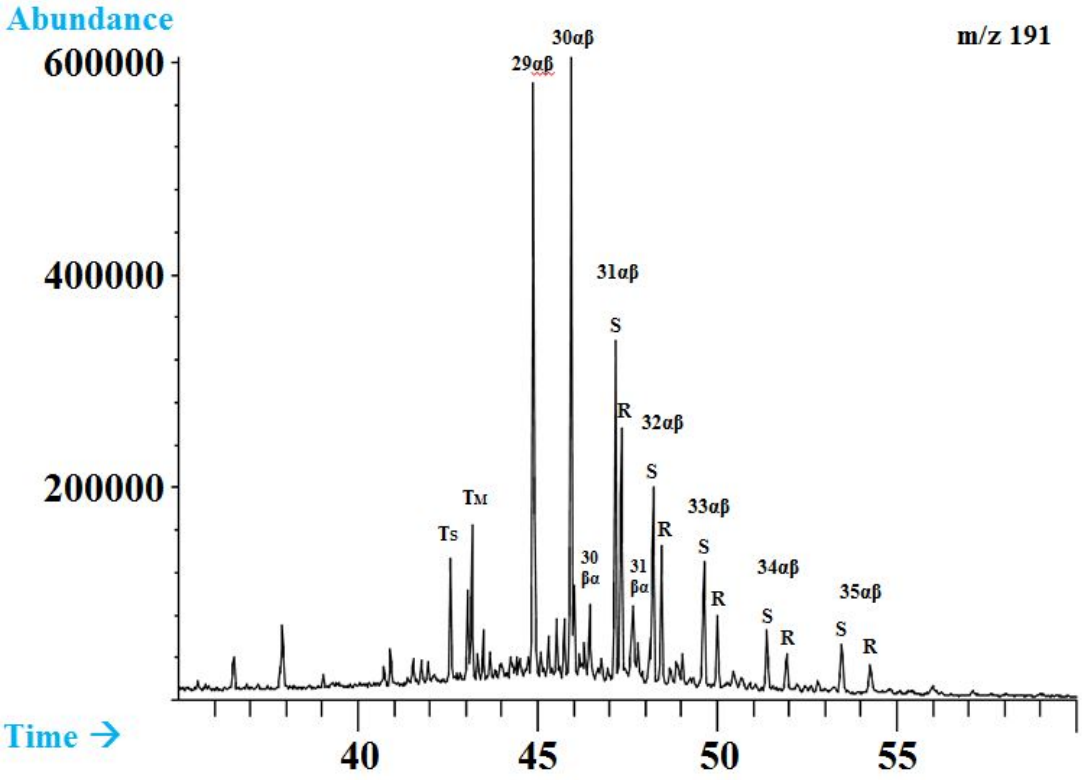

Figure 4.4 Characteristic ion fragmentogram (m/z 191). Numerals refer to carbon numbers of hopane series; αβ =17α(H),21β(H)-hopanes; βα =17β(H),21α(H)-hopanes; S and R = C_{22} S and R configuration; Ts: 18α(H)-22,29,30-trisnorneohopane; Tm: 17α(H)-22,29,30-trisnorhopane.

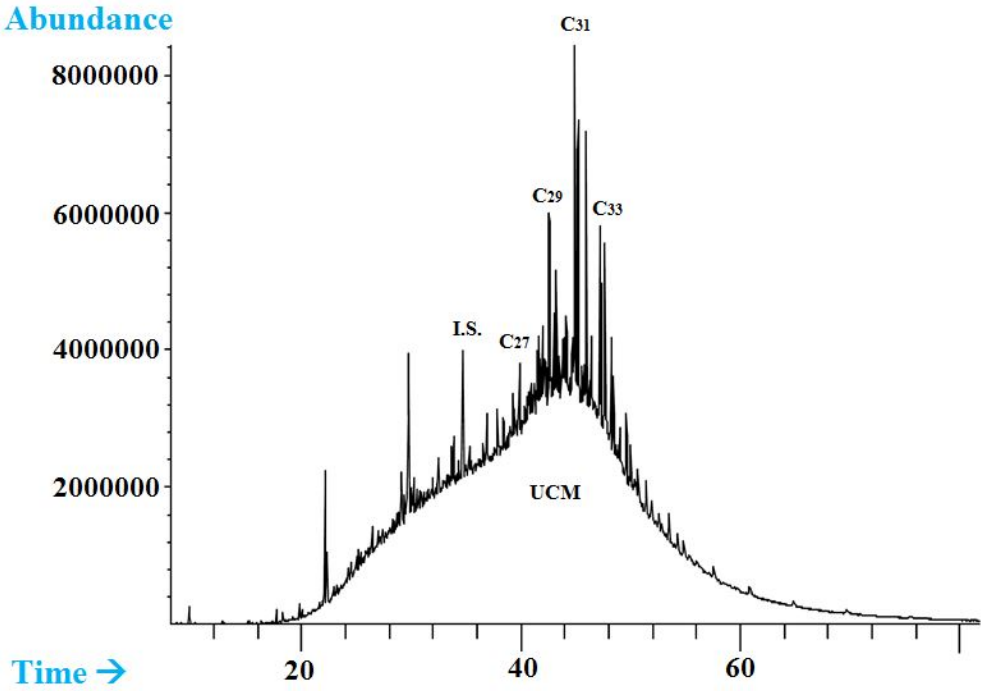

Figure 4.5 Characteristic chromatogram (full scan mode) of the upper part (0 cm depth) of WF-S2 core

The concentrations of the sum of *n*-alkanes vary between 0.53 and 4.37 μg g^{-1}. The mean value is 2.11 μg g^{-1}. Absolute (μg/g of dry sediment) concentrations of bias and non bias terrestrial *n*-alkanes are presented in Figure 4.6. The absolute concentrations range from 0.44 to 3.09 μg g^{-1} (bias) and from 0.39 to 2.45 μg g^{-1} (non bias). Figure 4.6 shows that the values of the absolute concentrations increase only slightly from the bottom of the core (around 1620 AD) until the last decades of the 19th century, having the minimum value 0.39 μg g^{-1}, maximum 2.45 μg g^{-1} and the mean value 0.86 μg g^{-1}. After that period and until today the increasing trend becomes radical and the values vary from 1.13 to 2.42 μg g^{-1} and the mean value is 1.85 μg g^{-1}.

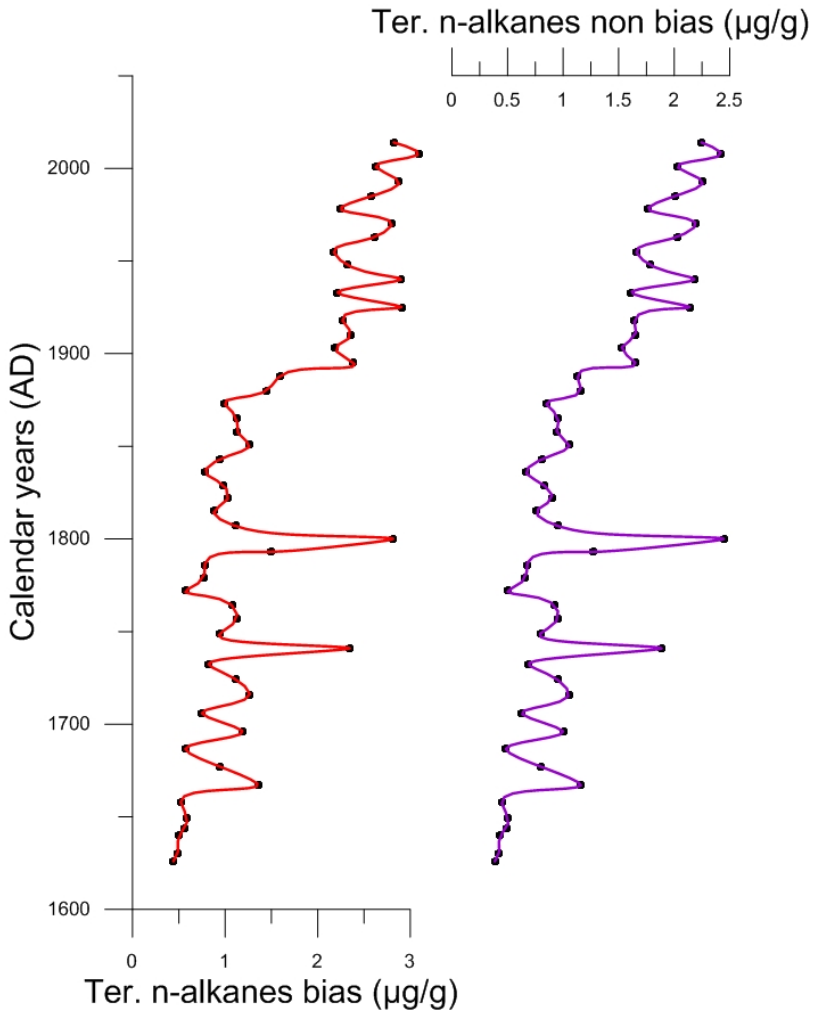

Figure 4.6 Absolute bias values of terrestrial *n*-alkanes (μg g^{-1}) and absolute non bias values (μg g^{-1}), respectively.

The CPI values of high molecular weight *n*-alkanes range from 2.89 to 7.36. From around 1620 AD till the last decades of the 19th century, CPI values have a mean value of 6.38. For the next three decades a sudden drop to a mean value of 3 is observed. After that and until today, CPI increases to the present value of 4.55.

UCM values vary between 7.87 and 600 μg g^{-1} (see Figure 4.7). The mean value is 178 μg g^{-1}. From around 1620 AD till the last decades of the 19th century, the values of UCM show a slightly increasing trend varying between 7.9 and 188 μg g^{-1}. After that period and until the middle of the 20th century, UCM increases from 180 to 600 μg g^{-1}. The last section demonstrates decreasing values for the UCM.

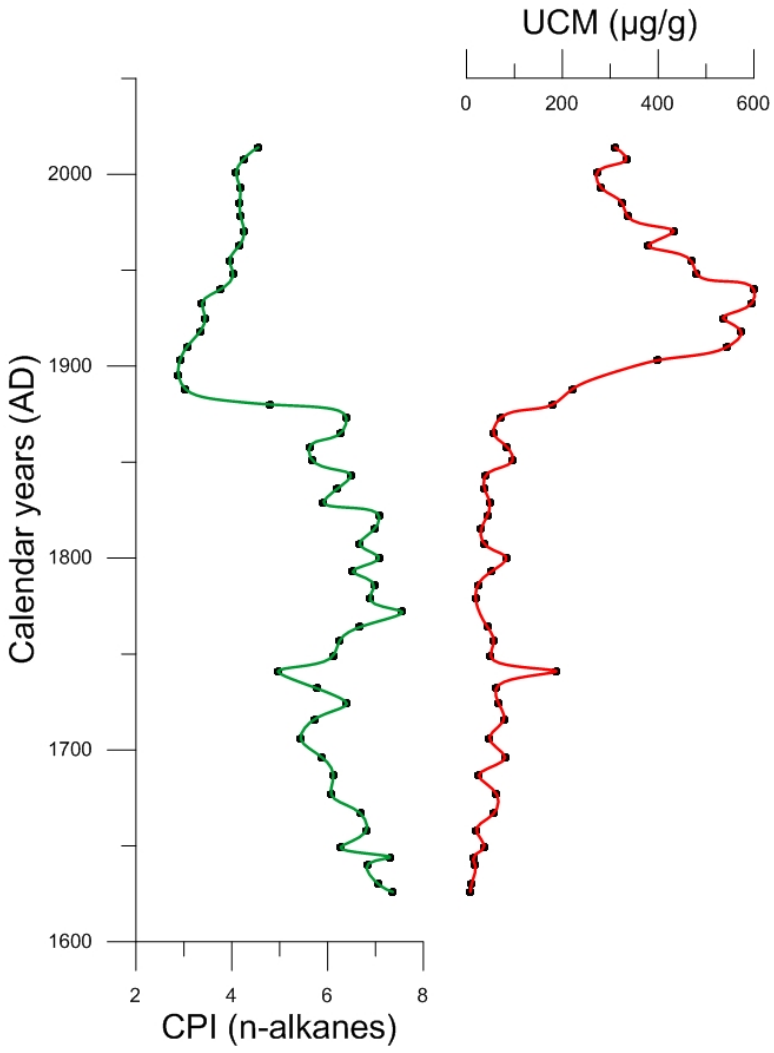

Figure 4.7 Carbon Preference Index (CPI) and Unresolved Complex Mixture (UCM) of long chain *n*-alkanes

The ACL index of *n*-C_{27} – *n*-C_{33} *n*-alkanes varies between 30.50 and 30.93 (see Figure 4.8). During the pre-Industrial period ACL values remain relatively constant. A decline in ACL values is observed during the last decades of the 19th century. Finally, from the onset of the 20th century till the middle of the century a rise in the values is noticed, while in the last decades the fluctuations appear to be more mild.

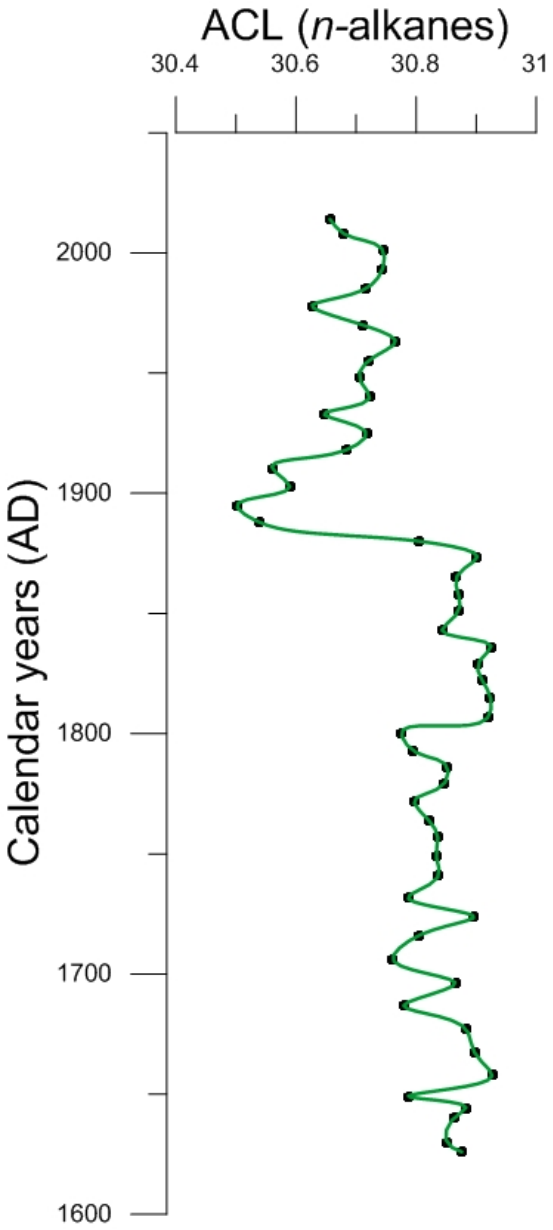

Figure 4.8 Average Chain Length (ACL) of C_{27} to C_{33} *n*-alkanes

4.4 Aliphatic alcohol fraction

The aliphatic alcohol fraction is dominated by a series of *n*-alkanols ranging from *n*-$C_{14\text{-OH}}$ to *n*-$C_{32\text{-OH}}$. The distribution of these compounds is dominated by even-carbon-number homologues with maxima at *n*-$C_{26\text{-OH}}$ or *n*-$C_{28\text{-OH}}$.

In Figure 4.9 a characteristic chromatogram of *n*-alkanols is presented. The dominant homologue is *n*-$C_{28\text{-OH}}$. Besides, even-carbon-number homologues ranging from *n*-$C_{24\text{-OH}}$ to *n*-$C_{32\text{-OH}}$ are dominant.

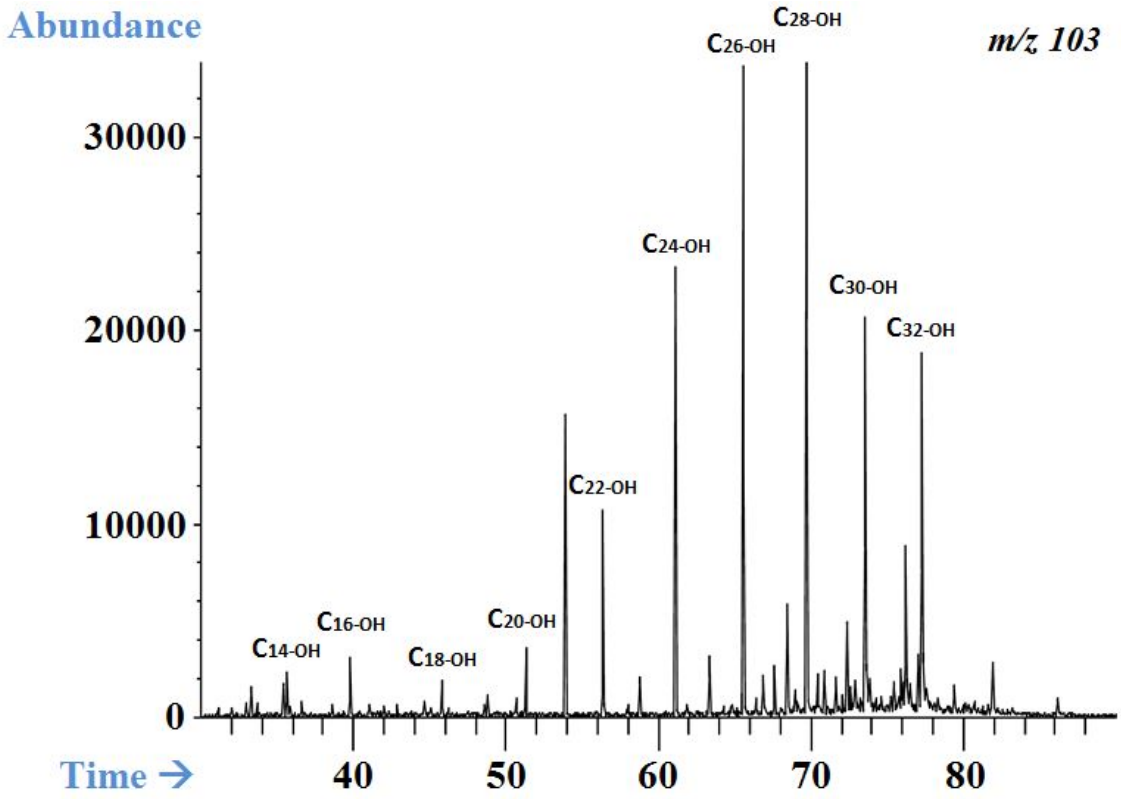

Figure 4.9 Characteristic chromatogram (*m/z 103*) of *n*-alkanols

Absolute (µg g^{-1} of dry sediment) and organic carbon normalized (µg g^{-1} of OC) concentrations of terrestrial *n*-alkanols are presented in Figure 4.10. Both absolute and organic carbon normalized values follow a similar distribution as the corresponding terrestrial *n*-alkanes. They range from 0.82 to 12.5 µg g^{-1} and from 91.2 to 351 µg g^{-1} OC respectively. For both graphs the

maximum values are observed at the top of the core (around 2010 AD), while the minimum at the bottom (around 1620 AD).

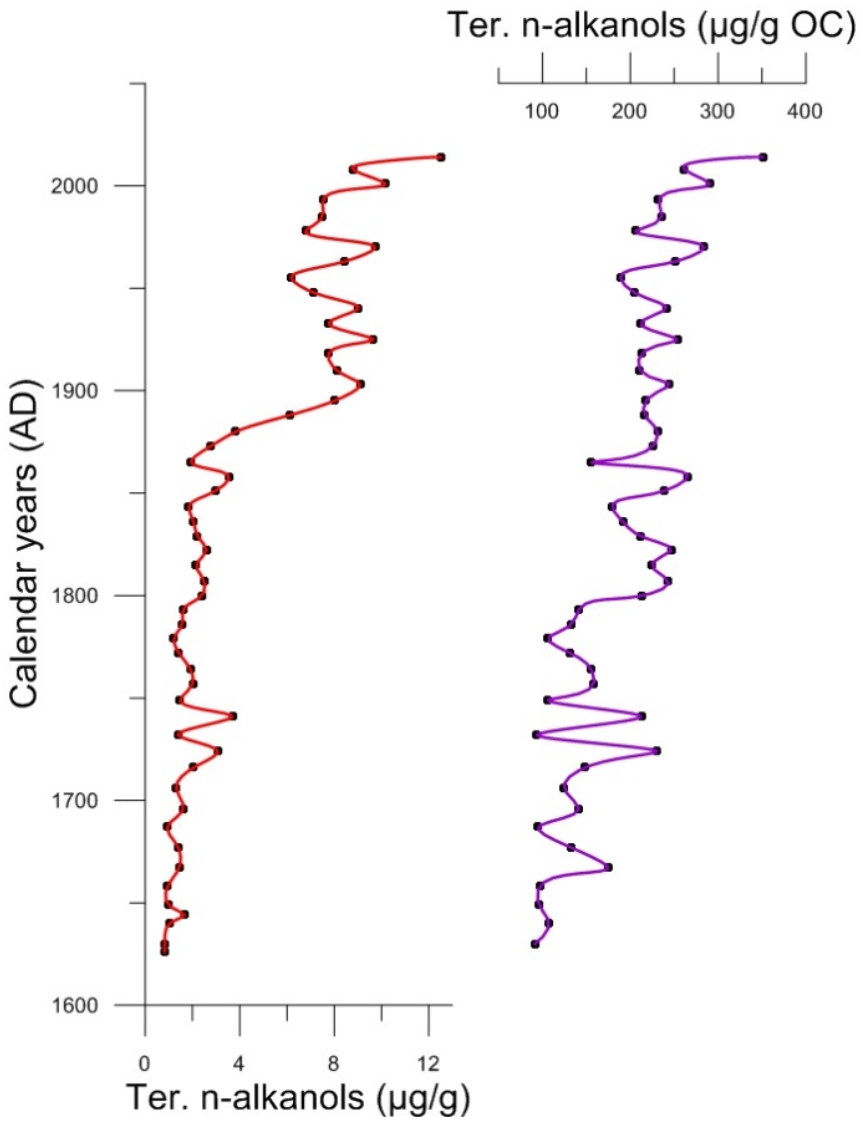

Figure 4.10 Absolute values of terrestrial *n*-alkanols (µg g^{-1}) and organic carbon normalized (µg g^{-1} OC), respectively.

It is generally accepted that the sums of even-carbon-number *n*-alkanols from *n*-C_{14} to *n*-C_{20} have marine origin [127]. Figure 4.11 shows that they vary between 0.06 and 4.46 µg g^{-1}.

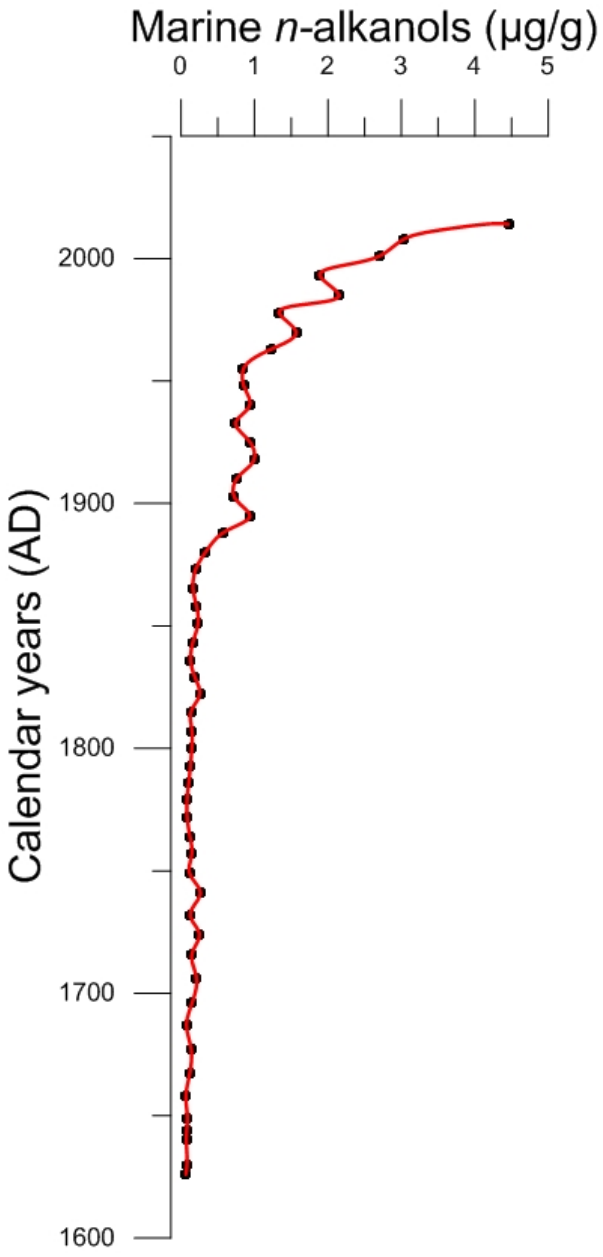

Figure 4.11 Absolute values of marine *n*-alkanols (µg g^{-1}).

4.5 Long-chain alkenones

Long-chain di- and tri-unsaturated C_{37} and C_{38} methyl ketones and C_{38} ethyl ketones (commonly named long-chain alkenones) were major components of the ketone fraction. In Figure 4.12 a characteristic chromatogram of the determined alkenones is depicted.

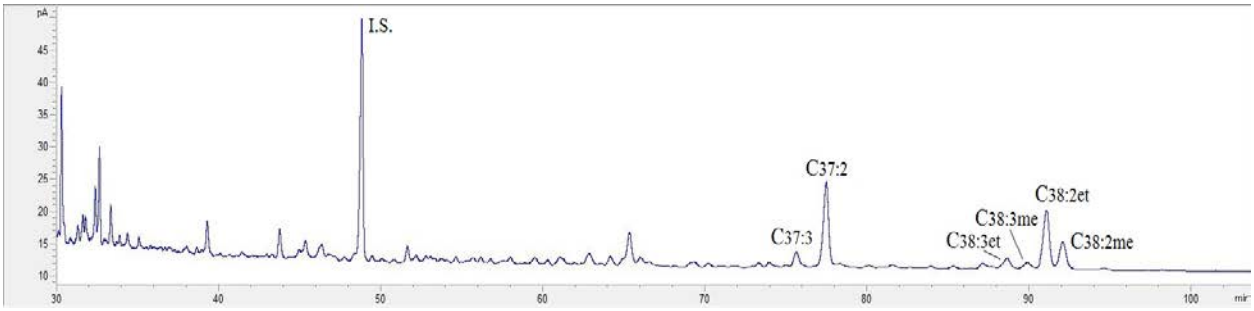

Figure 4.12 Characteristic chromatogram of alkenones

Their concentrations range from 0.16 to 10.64 μg g^{-1}. The minimum value of 0.16 μg g^{-1} is observed during the first decade of the 18th century, while the maximum of 10.64 μg g^{-1} during the last decades of the 19th century. From the end of the 17th century until the last decades of the 19th century, the total alkenone concentration values are quite low with a mean value 0.43 μg g^{-1}. After that period a sharp increase in values is observed, followed by a negative trend that continues till the top of the core (see Figure 4.13).

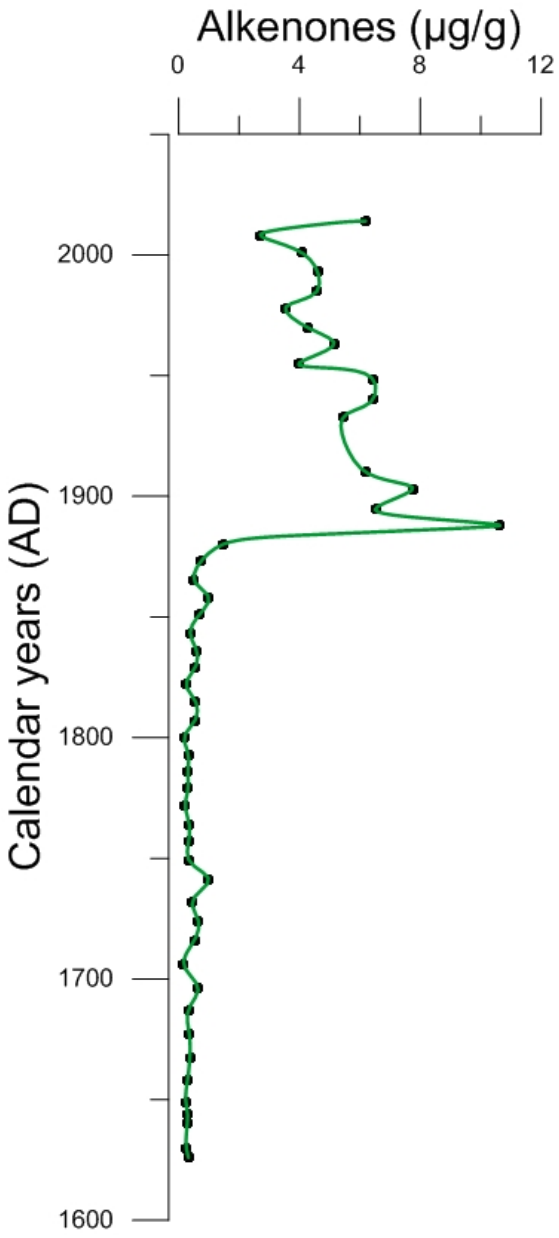

Figure 4.13 Alkenones concentration (µg g^{-1})

4.6 Sterols

The sterols determined in this study consist of a series of C_{26} – C_{29} 4-desmethyl sterols along with two C_{30} 4α-methyl sterols. The maximum values of total sterol concentration are found at the top of the core. In Figure 4.14 a characteristic chromatogram of sterols is presented. The dominant sterol is 4a,23,24-trimethyl-5a(H)cholest-22(E)-en-3β-ol (Dinosterol, $30\Delta^{22E}$). The sterols S13, S15, S16, S19 and S20 were not identified in any depth throughout the core.

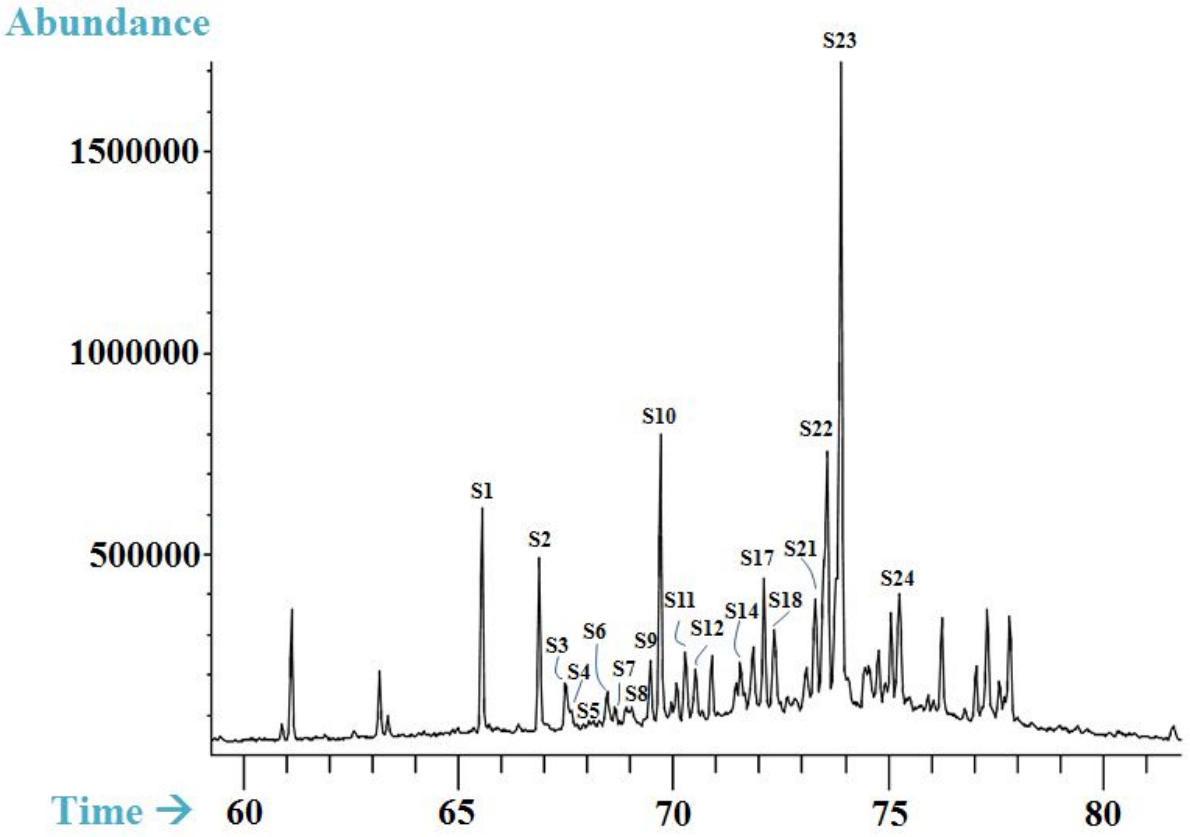

Figure 4.14 Characteristic total ion chromatograph (TIC) of suspended particle associated sterols (10cm) annotated with the identified compounds.

4.6.1 4-Desmethyl sterols

In all samples a series of C_{26}-C_{29} 4-desmethyl sterols have been detected (Table 3-2). C_{26} sterols, namely 24-norcholesta-5,22(E)-dien-3β-ol and 24-nor-5α(H)-cholest-22(E)-en-3β-ol were minor components accounting for less than 2% of the total sterol concentration.

C_{27} sterols account from 16% up to 31% of total sterol concentration. The major C_{27} sterol is cholest-5-en-3β-ol (cholesterol, $27\Delta^{5}$). Its dehydro-counterpart, cholesta-5,22(E)-dien-3β-ol ($27\Delta^{5,22E}$), as well as its hydrogenated one, 5α(H)-cholest-22(E)-en-3β-ol, are also present in low concentrations.

Three individual C_{28} sterols were identified accounting for 4 - 21% of the total sterols. The major C_{28} homologues are 24-methylcholesta-5,22-dien-3β-ol (Brassicasterol, $28\Delta^{5,22E}$) and 24-methylcholest-5-en-3β-ol (Campesterol, $28\Delta^{5}$).

As far as the C_{29}-sterols are concerned, 4 individual sterols are identified. The major C_{29} sterols are 24-ethylcholesta-5,22(E)-dien-3β-ol (Stigmasterol, $29\Delta^{5,22E}$) and 24-ethylcholesta-5-en-3β-ol (Sitosterol, $29\Delta^{5}$).

According to Figure 4.15, from the bottom of the core (2nd half of the 17th century) till the last decades of the 19th century, the major 4-desmethyl sterols average concentrations are lower than 0.15 μg g^{-1} (see Figure 4.15). After this turning point, that marks the beginning of the Industrial Era in Greece, all concentrations increase for the next decades.

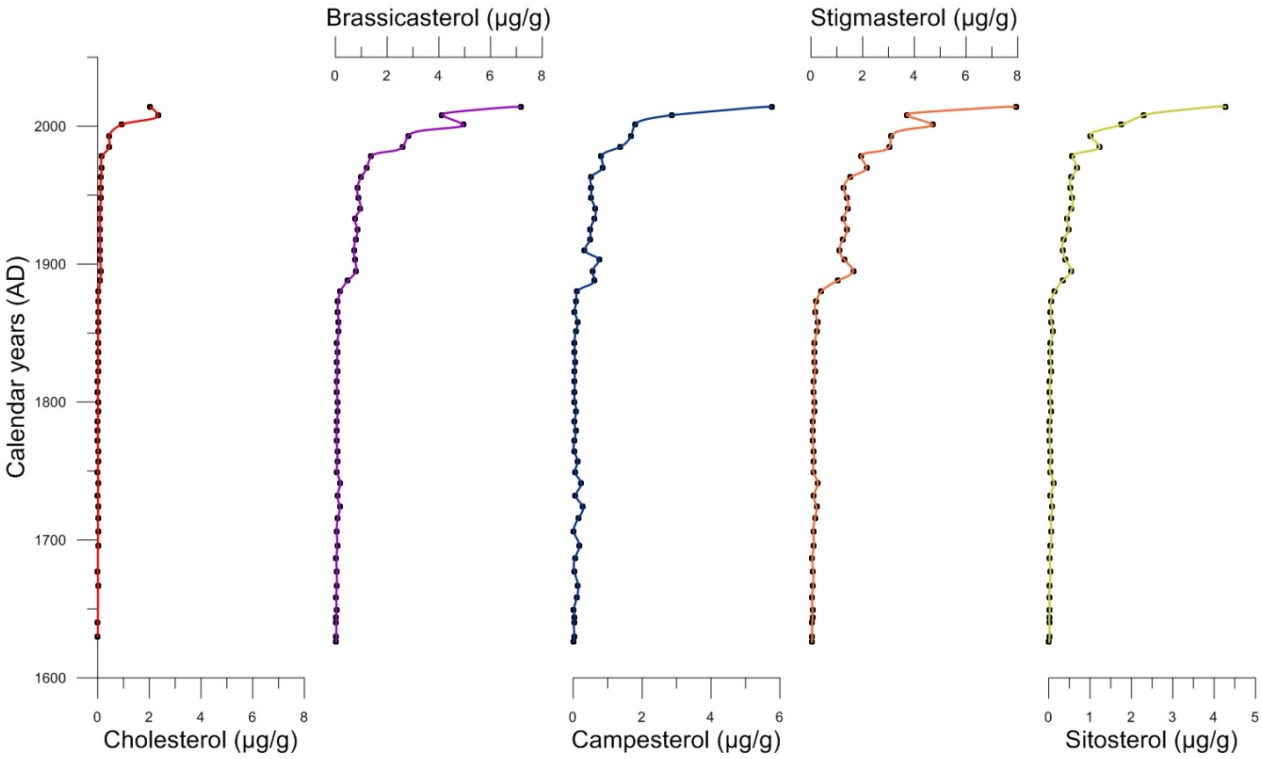

Figure 4.15 Major 4-desmethyl sterols concentrations

Figure 4.16 displays their vertical profiles. It is observed that the values of these two stanols rise after the last decades of the 19th centrury, compared to the very low concentrations demonstrated before this period.

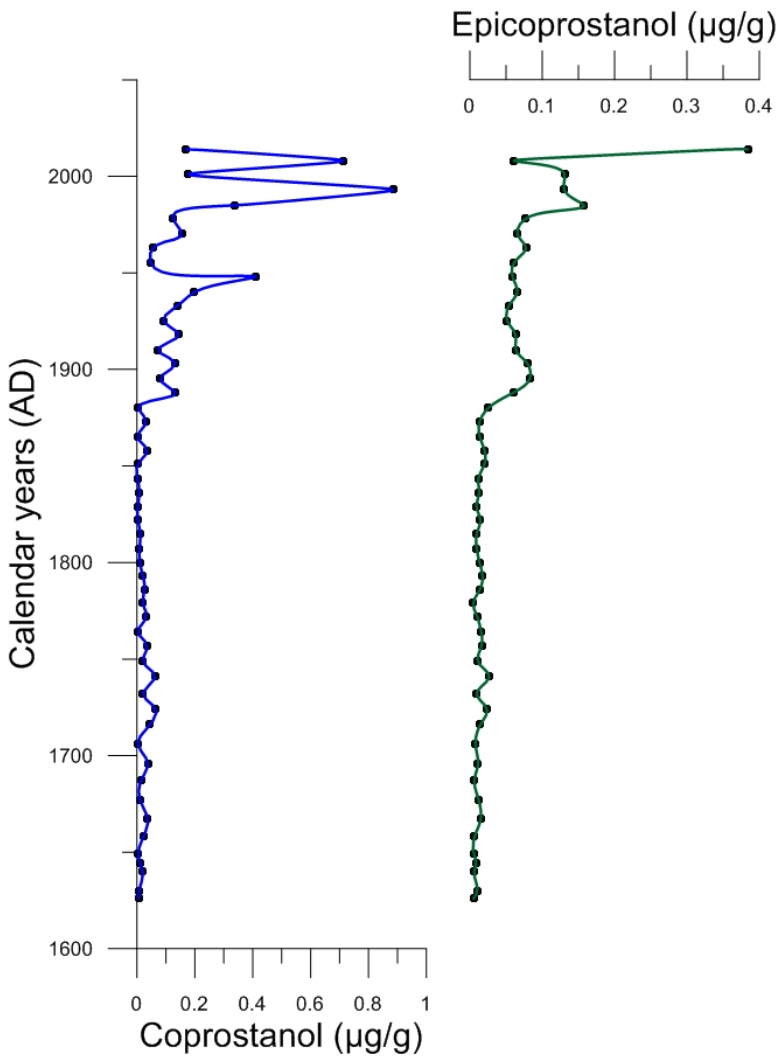

Figure 4.16 5β-cholestan-3β-ol (coprostanol) and 5β-cholestan-3α-ol (epicoprostanol) vertical profiles

4.6.2 4-Methyl sterols

4-methyl sterols are sterols with a methyl group at the 4-position. In this study, two C_{30} sterols are found. The major one is the 4a,23,24-trimethyl-5a(H)cholest-22(E)-en-3β-ol (Dinosterol, $30\Delta^{22E}$).

From the 2nd half of the 17th century until about the middle of the 19th century, 4a,23,24-trimethyl-5a(H)cholest-22(E)-en-3β-ol (Dinosterol, $30\Delta^{22E}$) concentration shows the mean value 0.44 µg g^{-1} (see Figure 4.17). A slight increase in its values is observed after that period and for the next decades. The last decades of the 19th century mark an immense increase of 4a,23,24-trimethyl-5a(H)cholest-22(E)-en-3β-ol (Dinosterol, $30\Delta^{22E}$) concentration. During the 20th

century the values exhibit fluctuations. Besides, the new millennia values have an increasing trend.

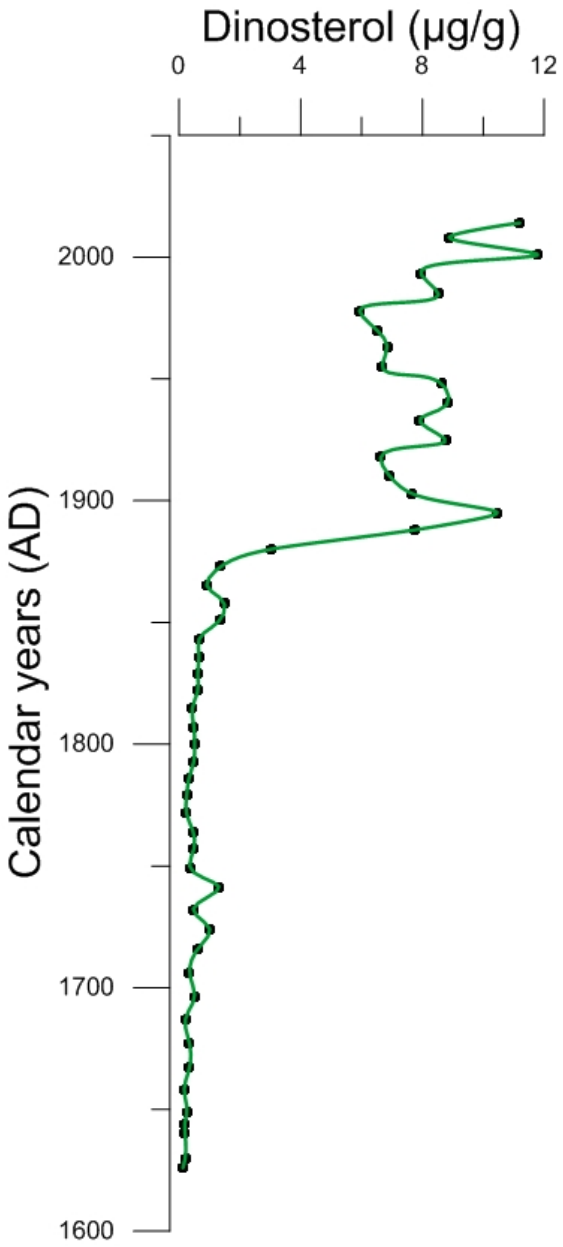

Figure 4.17 Dinosterol ($30\Delta^{22E}$) concentration

4.6.3 Algal productivity

The sum of algal biomarkers varies between 0.7 and 31.8 µg g^{-1} and has a mean value of 7.1 µg g^{-1}. As it is presented in Figure 4.18, from the bottom of the core until the last decades of 19th

century the vertical profile of ΣAlgal has almost constantly low values with mean value 1.7 μg g^{-1}. After that period and for the next decades, the values of ΣAlgal rise rapidly to 20.4 μg g^{-1}. During the 20th century there are some fluctuations in the concentration of ΣAlgal, but the general trend is increasing. The minimum value for this period is 13.5 μg g^{-1}, the maximum 31.8 μg g^{-1}, while the mean value is 18.6 μg g^{-1}.

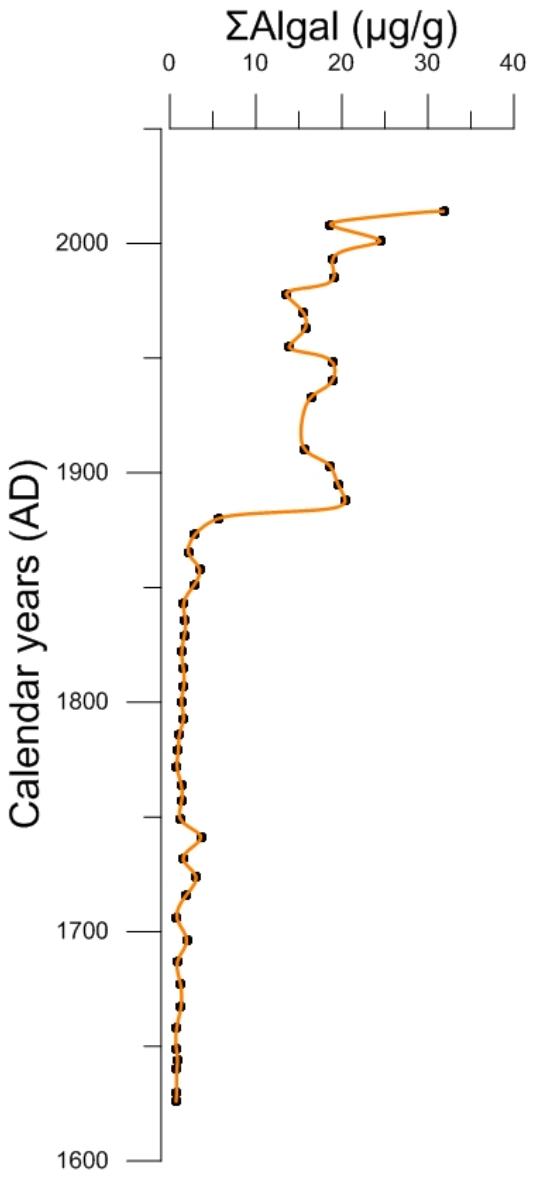

Figure 4.18 Total algal productivity concentration profile

4.7 PAH

Total PAH concentrations were calculated in 52 samples. The molecular profile of PAHs is depicted in Figure 4.19.

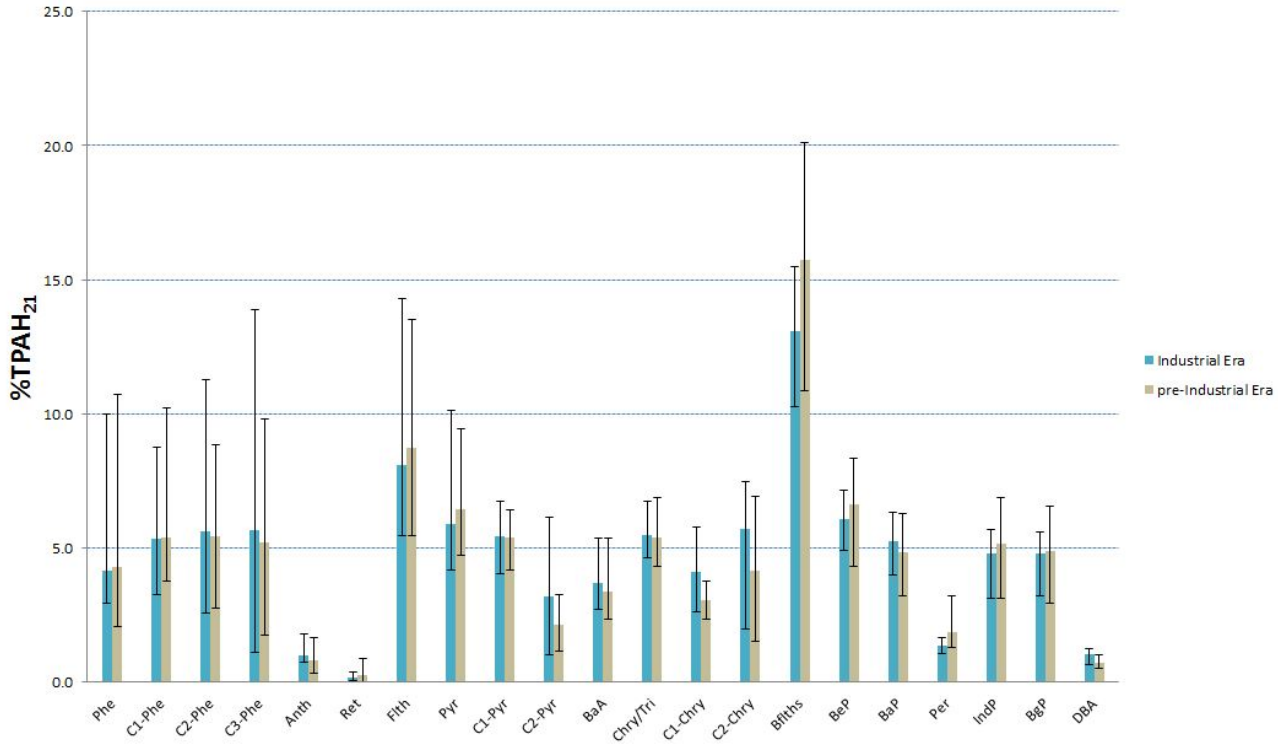

Figure 4.19 GC/MS profile of PAHs in the studied area. The profile illustrates the changes in composition downcore between the Industrial and pre-Industrial Era.

The depth profile is presented in Figure 4.20. The concentrations ranged between 50.6 and 2437.4 ng g^{-1}. From around 1620 AD until the middle of the 19th century the concentrations range between 50.6 and 1456.1 ng g^{-1}. The highest values were measured at the 14-18 cm (last decades of the 19th century) sediment layer, marking a peak since the concentrations below and above this layer are considerably lower. The upper 14 cm are characterized with PAH concentrations ranging between 1015.7 and 1874.9 ng g^{-1}.

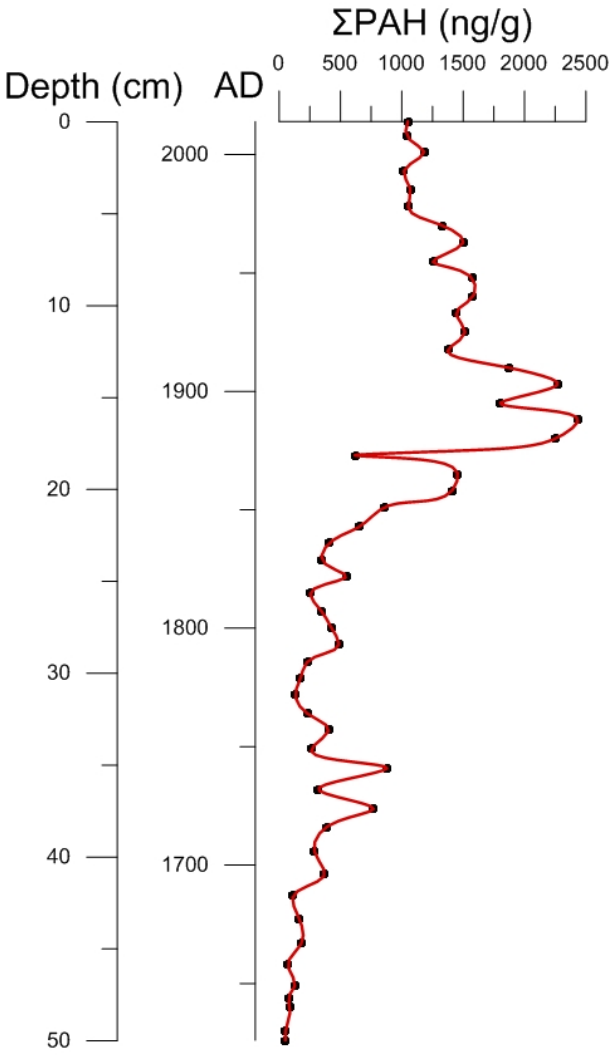

Figure 4.20 Total PAHs concentration profile

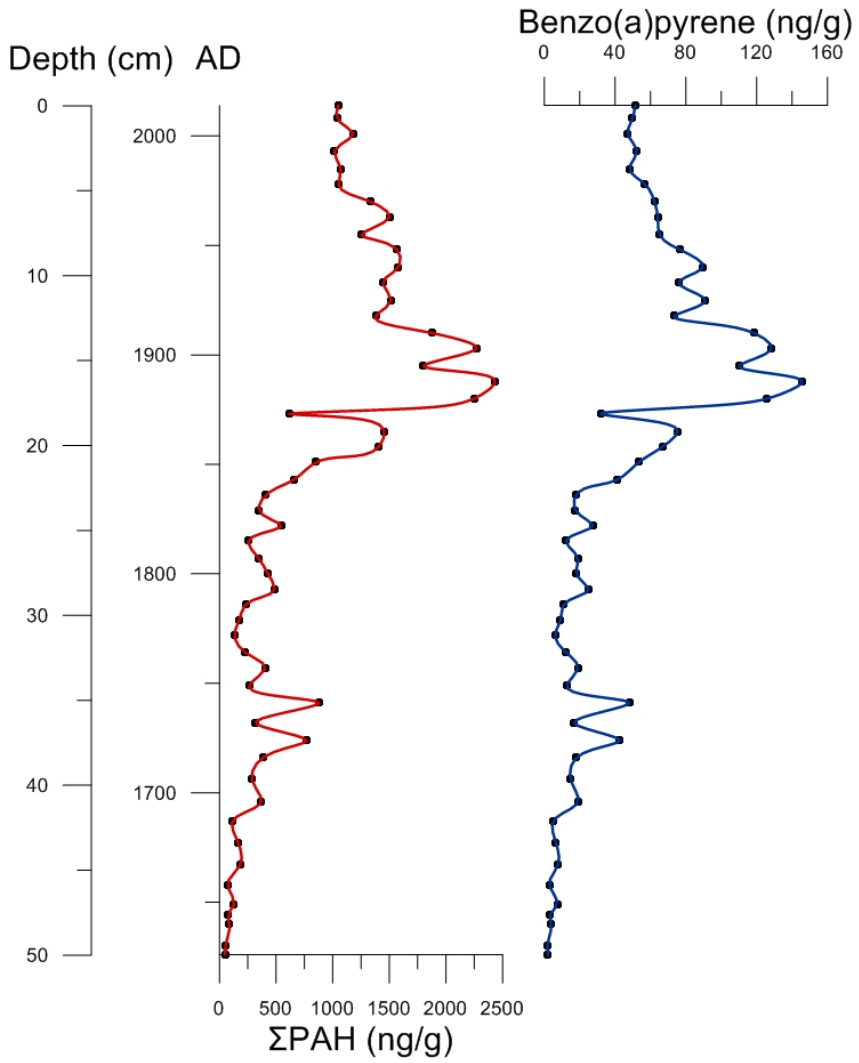

Figure 4.21 Benzo(a)pyrene concentration profile correlated with ΣPAH profile.

5 DISCUSSION

The approach adopted here uses selected marine and terrestrially derived biogeochemical indices retrieved from the WF-S2 sedimentary record and focuses on the identification of land-sea climate interactions and the sensitivities and response modes to temperature and hydrological changes concerning the Saronikos Gulf during the last 300 years. The study of WF-S2 core reveals a radical rise in OC (Figure 4.2) and UCM (Figure 4.7) values in parallel with a significant decrease in CPI (Figure 4.7) values during the last decades of the 19th century. These results are consistent with previous studies [106], [147]. Thus, the core is divided into two different periods, i.e. before and after the beginning of the Industrial Era.

5.1 Pre-Industrial period

Proxy-reconstructions of the WF-S2 record reveal an SST cooling trend of almost 1^{o}C from the first quarter of the 17th century to the beginning of the 18th century. This cooling is probably synchronous to one of the coldest intervals (ad 1645–1715) of the 'Little Ice Age' (LIA), characterized by a prolonged episode of volcanic and low solar activity known as 'Maunder minimum' (MM) [28][148], [149]. During the same period and until the middle of the 18th century, relatively higher concentrations of terrestrial biomarkers (Terrestrial *n*-alkanes and *n*-alkanols), slightly higher organic carbon content (OC) and depleted δ^{13}C values, suggest higher supply from continental/riverine runoffs to the marine site [124], [127], [150], [151].

Throughout the 18th century SSTs stabilize at a mean temperature of 23^{o}C. At ca 1770 a sudden drop of 1^{o}C is observed. This is probably the result of a previous hydrological change at ca 1740, pinpointing to enhanced inputs from the the surrounding land, as suggested by the sudden rise of terrestrial (Ter-alkanes and –alkanols) and marine (alkenones, sterols and marine *n*-alkanols) biomarkers concentrations as also as by the depleted δ^{13}C values. This "event" is also illustrated by peaking of the ΣPAH values.

A positive trend in SSTs starts at the beginning of the 19th century. Relatively high δ^{13}C values, increased concentrations of *n*-alkanes consistent with rising total PAH (ΣPAH) values, suggest the enlargement of the settlements of the area and probably increased wood burning, the result of fires during this turbulent period in the history of the area.

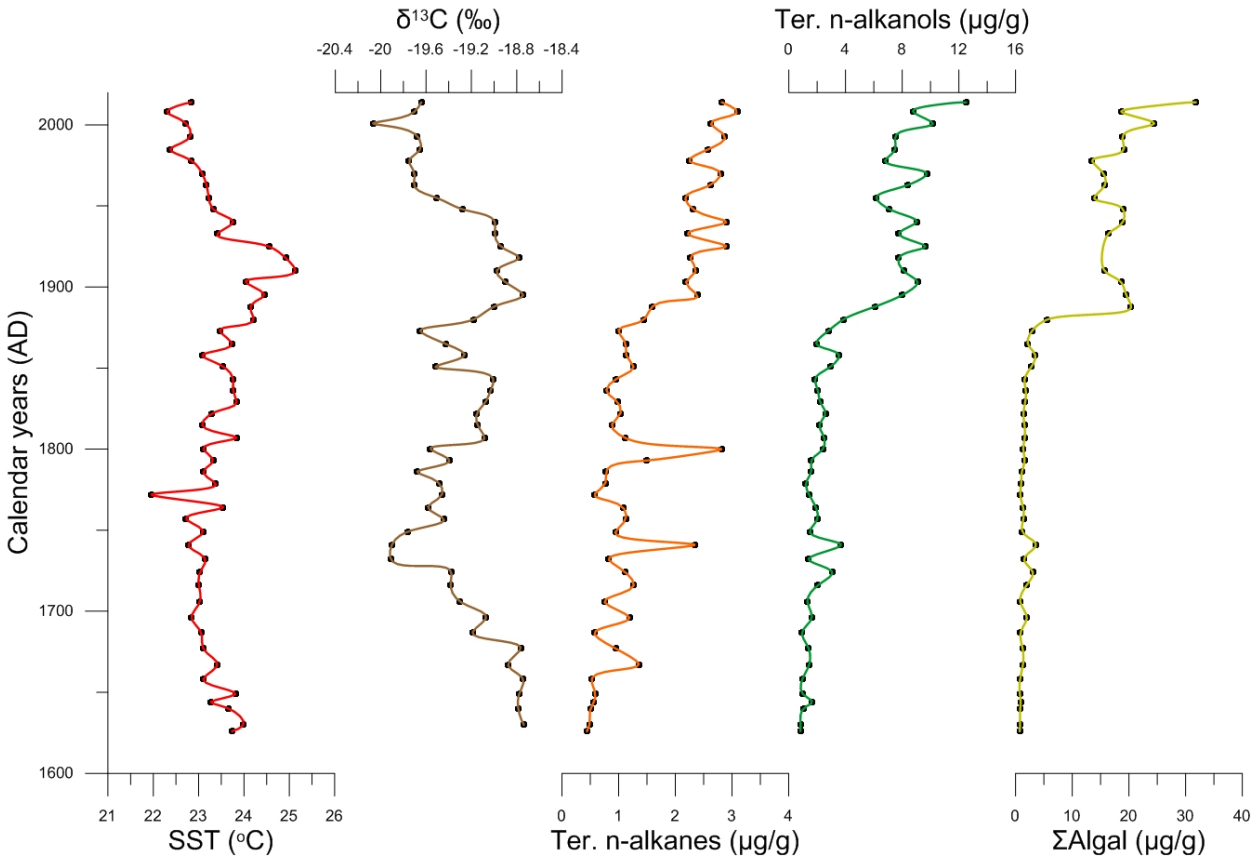

Figure 5.1 Sea Surface Temperatures, $\delta^{13}C$ values and lipid biomarkers' concentrations vs. calibrated age along WF-S2 core

5.2 Industrial period

During the last decades of the 19th century the SSTs increase by 1°C in just a few decades. The maximum value of 25.1°C is observed at ca 1910. The radical increase of the values of organic carbon content (OC) and the simultaneous decreasing mode of the $\delta^{13}C$ values (Figure 5.1), showing relative increase in the supply of terrigenous matter in the core site, suggest the beginning of the Industrial Era in Greece but also the rise of the surrounding area population as published in Papaioannou et *al.* [149]. This is in accordance with previous studies in the area [106], [152] and it is attributed to the hydrological characteristics of the bay that favor the trapping and accumulation of organic rich particulates to the western part of the area which is also the deepest point of the bay.

From ca. 1880 to 1940 AD, the values of UCM increase from 180 to 600 μg g^{-1}. This radical increase of the UCM indicates the accumulation of chronic pollution in the sediments. This is the

result of the degradation process of aliphatic compounds of crude oil and petroleum products released in marine environments, attributed to the prominent initial microbial preference for straight-chain compounds [53]. The gradual removal of these major compounds that can be resolved by gas chromatography and concludes to the appearance of the UCM, consists of branched alicyclic hydrocarbons that persist in sediments for decades [135]. Further verification of entering an era of higher anthropogenic activity is provided by the CPI_{NA} index. As Figure 1.2 depicts, the CPI values drop to less than 4. These low values show the impact of fossil fuel burning, while values >4 are consistent with a terrestrial origin from land plants [153].

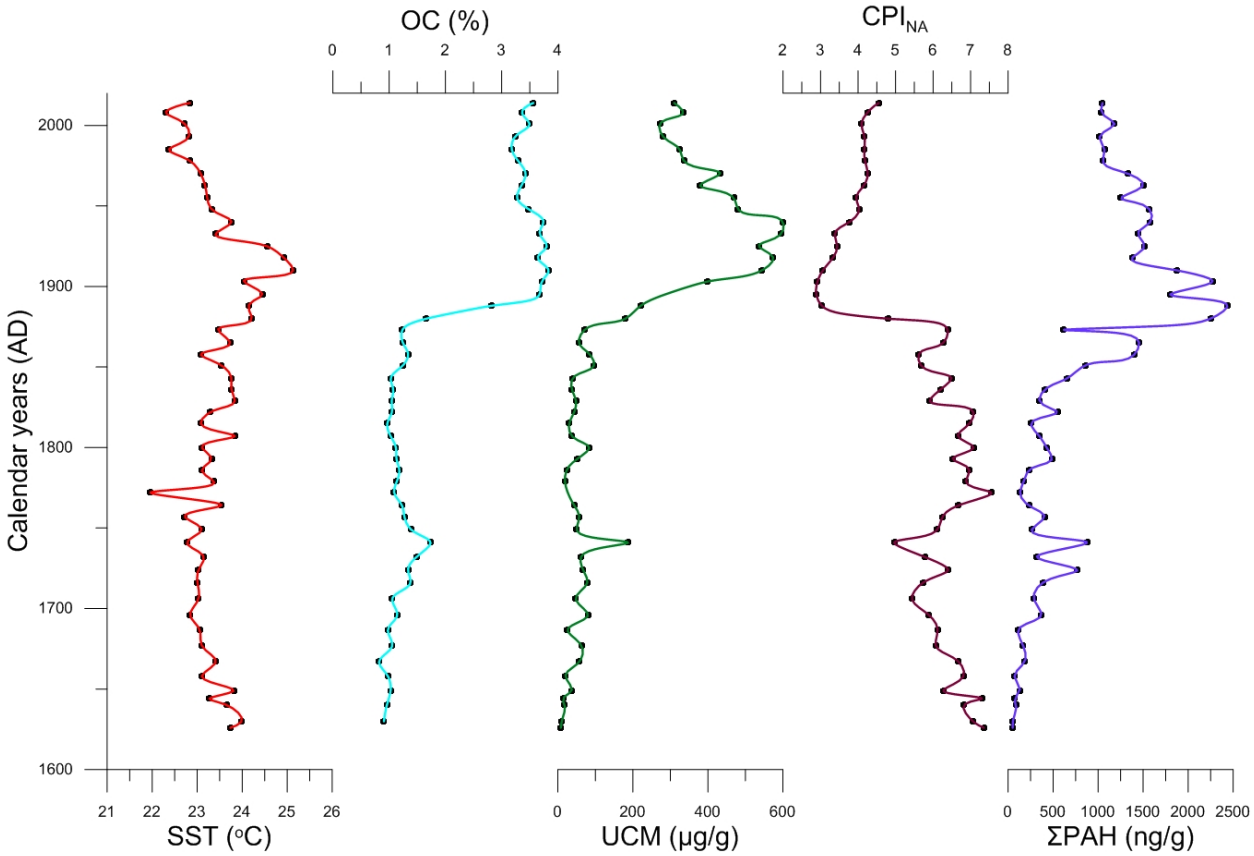

Figure 1.2 Sea Surface Temperatures, OC contents, total PAH concentrations and indices vs. calibrated age along WF-S2 core

Overall enhanced inputs from the surrounding land is evidenced by enhanced terrigenous inputs (Terrestrial *n*-alkanes and *n*-alkanols). The concomitant supply of nutrients to the marine site supports higher rates of algal productivity in the euphotic zone, as witnessed by rise of ΣAlgal, higher OC values and shift of $\delta^{13}C$ towards higher values.

5β-cholestan-3β-ol (coprostanol) and 5β-cholestan-3α-ol (epicoprostanol) consist the products of most higher animals and birds. These compounds have frequently been used as a biomarkers for the presence of human and animal faecal matter in the environment [154]. As Figure 4.16 shows, during the same period the radical rise of the values of both sterols indicates the rising of the population of the surrounding area [155], having as a consequence the higher concentration of faecal matter in the marine environment.

As Figure 1.2 depicts, the beginning of the Industrial Era correlates well with the sudden rise of total PAH concentration (ΣPAH) from 617.6 ng g^{-1} (pre-Industrial value) to a maximum value of 2437.4 ng g^{-1}. The above observation is consistent with previous studies in the area [106] and the eastern Mediterranean [147], which present a peak of ΣPAH values around the same time. Papaioannou *et al.* [148], [149] suggest a *Pinus* retreat after the second half of the 19th century, probably the result of a rising population with higher demands in wood burning.

A negative trend in SSTs starts at the beginning of the 20th century and continues until today. It is probably the result of a combination of events that have thereafter affected temperature and probably other physicochemical characteristics of the study area. The higher concentrations of terrestrial biomarkers and depleted values of $\delta^{13}C$, suggest higher supply from continental runoffs. At the same time, higher concentrations of marine *n*-alkanols consistent with a marine derived sterol (a.k.a. dinosterol) presumably triggered by increases in nutrient availability, further support the hypothesis of enhanced continental inputs during this time. Also the concurrent negative trend in ΣPAH values seems to conform with the gradual replacement of coal-based fuels to petroleum and natural gas, as Azoury *et al.*[147] have suggested. The influence of coal combustion on PAH emissions is also relatively well demonstrated by several historical records in marine and lake sediments in North America and in Western Europe [156]–[163].

5.3 Other proxies indicating petrogenic or pyrolytic origin

Depending on their origins, polycyclic aromatic hydrocarbons (PAH) are characterized by different chemical properties. Petrogenic PAH originate from fossil fuels while pyrolytic PAH are commonly produced by incineration processes.

Besides, a range of diagnostic ratios of specific PAHs has been used, in order to succeed a more reliable distinguish between combustion and petroleum sources [164]. For molecular weight 228, the ratio of benzo(a)anthracene to benzo(a)anthracene plus chrysene [BaA/(BaA+Chry)]. Values of this ratio <0.20 likely indicate petroleum, whereas values >0.35 imply combustion sources [164]. The values of the ratio varied between 0.32 and 0.44, supporting the combustion origin of PAHs. As far as the higher molecular weight PAHs (276) is concerned, the values of the ratio of indeno(1,2,3-c,d)pyrene to indeno(1,2,3-c,d)pyrene plus benzo(g,h,i)perylene [IndP/(IndP+BgP)] varied between 0.48 to 0.54 with a mean value of 0.51. This observation further indicates pyrolytic sources throughout the whole core, as Yunker *et al.* [164] suggest that the values of this ratio above 0.5 imply combustion sources. In the case of Elefsis Bay the vertical profiles of these ratios are presented in Figure 1.3.

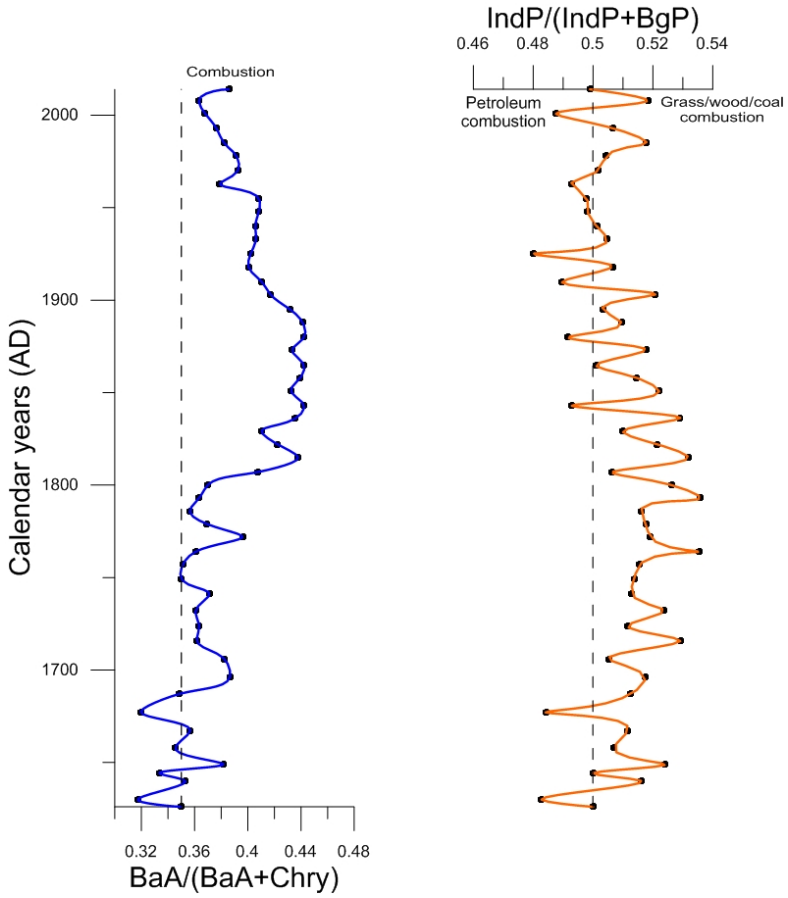

Figure 1.3 Benzo(a)anthracene to benzo(a)anthracene plus chrysene and indeno(1,2,3-c,d)pyrene to indeno(1,2,3-c,d)pyrene plus benzo(g,h,i)perylene ratios

The origin of PAHs is attributed to a mixed contribution from both fossil and pyrolytic sources, as deduced from their molecular profile (Figure 4.19) and source-specific indices.

In the samples analyzed benzofluoranthenes, benzo(e)pyrene, fluoranthene and pyrene were always predominant. These compounds are known to be of pyrolytic origin [106]. Benzo(a)pyrene, which has strong carcinogenic properties, was detected in all samples, even at the bottom of the core. The profile exhibits a similar behavior to that of the total PAHs (see Figure 4.21).

6 CONCLUSIONS

6.1 Concluding remarks

The present palaeoceanographic study for the last 300 years in Elefsis Bay based on multi-proxy reconstructions from the WF-S2 high resolution marine multi-core focuses on the land-sea climate interactions, the sensitivities and response-modes to temperature and hydrological changes and the human pressures on the environment. The present study can be divided into two different periods, the pre-industrial period and the industrial one, with the following observations:

- The pre-industrial period lasts until the last decades of the 19th century. From the first quarter of the 17th century to the beginning of the 18th century a cooling trend of SSTs is observed. During the same period it seems to have a higher supply from continental/riverine runoffs. Throughout the 18th century SSTs stabilize at a mean temperature of 23^{o}C and the values of the various biomarkers are almost constant. At the beginning of the 19th century the SSTs values show a rising trend and a series of proxies indicate the enlargement of the settlements of the surrounding area and the increased wood burning.
- The industrial period, beginning at the last decades of the 19th century, is apparent by almost all proxies. The SSTs increase by 1^{o}C in just a few decades. The rise of the population of the surrounding area and the overall enhanced inputs of terrestrial matter from the surrounding land is also evident through the increased export of all terrestrial biomarkers of biogenic and anthropogenic origin to the core site. During the 20th century a decreasing trend of the various pollution indices is observed which seems to conform with the gradual replacement of coal-based fuels to petroleum and natural gas.
- The origin of PAHs is attributed to a mixed contribution from both fossil and pyrolytic sources, as deduced from their molecular profile and source-specific indices.
- The decreasing trend of SSTs during the 20th century, at first glance, seems to be contradictory to the general warming trend of the last century. The trend is probably the result of the documented anoxic conditions that occur in the Elefsis Bay. Also, the decreasing SSTs show that the stratification is becoming stronger, as a result of the higher temperatures of the atmosphere, due to the climate change.

6.2 Future perspectives

- It is of high importance to focus more on coastal regions next to large metropolitan areas, where transport mechanisms appear to be rather complex and the environmental pressures from human activity are greater.

- Further studies in the Saronikos Gulf/ Elefsis Bay (included the WF-S2 core site) in order to support the present study. Specifically, there is a need for:

- micropaleontological study and $\delta^{18}O$ on biogenic carbonates in order to reconstruct past productivity and salinity changes
- air temperature and rainfall data in the study area so as to find the fresh water inputs per period.
- and other historical data e.g. records of flood events and land-use changes for the better understanding of the prevailing environmental conditions in the Thriasian Plain during the last 300 years.
- Pb isotopic composition analyses for a more accurate age-depth model and also in order to achieve a more accurate distinction between the different combustion sources.

7 REFERENCES

[1] K. Z. Allen, M.R., O.P. Dube, W. Solecki, F. Aragón-Durand, W. Cramer, S. Humphreys, M. Kainuma, J. Kala, N. Mahowald, Y. Mulugetta, R. Perez, M. Wairiu, “Global Warming of 1.5°C. An IPCC Special Report on the impacts of global warming of 1.5°C above pre-industrial levels and related global greenhouse gas emission pathways, in the context of strengthening the global response to the threat of climate change,” 2018.

[2] IPCC, “Climate Change Synthesis Report,” 2014.

[3] P. Lionello *et al.*, “The Mediterranean climate: An overview of the main characteristics and issues,” 2006, pp. 1–26.

[4] B. Ulbrich, U., Lionello, P., Belušić, D., Jacobeit, J., Knippertz, P., Kuglitsch, F.G., Leckebusch, G.C., Luterbacher, J., Maugeri M., Maheras, P., Nissen, K.M., Pavan, V., Pinto, J.G., Saaroni, H., Seubert, S., Toreti, A., Xoplaki, E., Ziv, “Climate of the Mediterranean: synoptic patterns, temperature, precipitation, winds and their extremes.,” in *The Climate of the Mediterranean region: from the past to the future.*, P. Lionello, Ed. 2012, pp. 301–346.

[5] E. Xoplaki, J. González-Rouco, D. Gyalistras, J. Luterbacher, R. Rickli, and H. Wanner, “Interannual summer air temperature variability over Greece and its connection to the large-scale atmospheric circulation and Mediterranean SSTs 1950–1999,” *Clim. Dyn.*, vol. 20, no. 5, pp. 537–554, Mar. 2003.

[6] E. Xoplaki, J. F. González-Rouco, J. Luterbacher, and H. Wanner, “Mediterranean summer air temperature variability and its connection to the large-scale atmospheric circulation and SSTs,” *Clim. Dyn.*, vol. 20, no. 7–8, pp. 723–739, May 2003.

[7] E. Xoplaki, J. F. González-Rouco, J. Luterbacher, and H. Wanner, “Wet season Mediterranean precipitation variability: influence of large-scale dynamics and trends,” *Clim. Dyn.*, vol. 23, no. 1, pp. 63–78, Aug. 2004.

[8] S. Brönnimann, E. Xoplaki, C. Casty, A. Pauling, and J. Luterbacher, “ENSO influence on Europe during the last centuries,” *Clim. Dyn.*, vol. 28, no. 2–3, pp. 181–197, Dec. 2006.

[9] S. A. Josey, S. Somot, and M. Tsimplis, “Impacts of atmospheric modes of variability on Mediterranean Sea surface heat exchange,” *J. Geophys. Res.*, vol. 116, no. C2, p. C02032, Feb. 2011.

[10] J. López-Parages and B. Rodríguez-Fonseca, “Multidecadal modulation of El Niño influence on the Euro-Mediterranean rainfall,” *Geophys. Res. Lett.*, vol. 39, no. 2, p. n/a-n/a, Jan. 2012.

[11] P. Malanotte-Rizzoli *et al.*, “Physical forcing and physical/biochemical variability of the Mediterranean Sea: a review of unresolved issues and directions for future research,” *Ocean Sci.*, vol. 10, no. 3, pp. 281–322, May 2014.

[12] M. V. Triantaphyllou *et al.*, “Holocene Climatic Optimum centennial-scale paleoceanography in the NE Aegean (Mediterranean Sea),” *Geo-Marine Lett.*, vol. 36, no. 1, pp. 51–66, 2016.

[13] M. Loizidou, C. Giannakopoulos, M. Bindi, and K. Moustakas, “Climate change impacts and adaptation options in the Mediterranean basin,” *Reg. Environ. Chang.*, vol. 16, no. 7, pp. 1859–1861, Oct. 2016.

[14] J. Guiot and W. Cramer, “Climate change: The 2015 Paris Agreement thresholds and Mediterranean basin ecosystems,” *Science (80-.).*, vol. 354, no. 6311, pp. 465–468, Oct. 2016.

[15] C. Katrantsiotis, “Holocene environmental changes and climate variability in the Eastern Mediterranean: Multiproxy sediment records from the Peloponnese peninsula, SW Greece,” 2019.

[16] I. Dormoy *et al.*, “Terrestrial climate variability and seasonality changes in the Mediterranean region between 15000 and 4000 years BP deduced from marine pollen records,” *Clim. Past Discuss.*, vol. 5, no. 1, pp. 735–770, Feb. 2009.

[17] M. Finné, K. Holmgren, H. S. Sundqvist, E. Weiberg, and M. Lindblom, “Climate in the eastern Mediterranean, and adjacent regions, during the past 6000 years – A review,” *J. Archaeol. Sci.*, vol. 38, no. 12, pp. 3153–3173, Dec. 2011.

[18] N. Roberts *et al.*, “Palaeolimnological evidence for an east–west climate see-saw in the Mediterranean since AD 900,” *Glob. Planet. Change*, vol. 84–85, pp. 23–34, Mar. 2012.

[19] M. Magny *et al.*, “North–south palaeohydrological contrasts in the central Mediterranean during the Holocene: tentative synthesis and working hypotheses,” *Clim. Past*, vol. 9, no. 5, pp. 2043–2071, Sep. 2013.

[20] O. Peyron *et al.*, “Contrasting patterns of climatic changes during the Holocene across the Italian Peninsula reconstructed from pollen data,” *Clim. Past*, vol. 9, no. 3, pp. 1233–1252, Jun. 2013.

[21] J. Luterbacher *et al.*, “A Review of 2000 Years of Paleoclimatic Evidence in the Mediterranean,” in *The Climate of the Mediterranean Region*, Elsevier, 2012, pp. 87–185.

[22] E. J. Rohling, G. Marino, and K. M. Grant, “Mediterranean climate and oceanography, and the periodic development of anoxic events (sapropels),” *Earth-Science Rev.*, vol. 143, pp. 62–97, Apr. 2015.

[23] J. Seguin *et al.*, “2500 years of anthropogenic and climatic landscape transformation in the Stymphalia polje, Greece,” *Quat. Sci. Rev.*, vol. 213, pp. 133–154, Jun. 2019.

[24] J. Esper, D. Frank, U. Büntgen, A. Verstege, J. Luterbacher, and E. Xoplaki, “Long-term drought severity variations in Morocco,” *Geophys. Res. Lett.*, vol. 34, no. 17, p. L17702, Sep. 2007.

[25] E. R. Cook *et al.*, “Old World megadroughts and pluvials during the Common Era,” *Sci. Adv.*, vol. 1, no. 10, p. e1500561, Nov. 2015.

[26] B. I. Cook, K. J. Anchukaitis, R. Touchan, D. M. Meko, and E. R. Cook, “Spatiotemporal drought variability in the Mediterranean over the last 900 years,” *J. Geophys. Res. Atmos.*, vol. 121, no. 5, pp. 2060–2074, Mar. 2016.

[27] J. Luterbacher, “European Seasonal and Annual Temperature Variability, Trends, and Extremes Since 1500,” *Science (80-.).*, vol. 303, no. 5663, pp. 1499–1503, Mar. 2004.

[28] H. Xoplaki, E.; Luterbacher, J.; Paeth, H.; Dietrich, D.; Steiner, N.; Grosjean, M.; Wanner, “European spring and autumn temperature variability and change of extremes over the last half millennium,” *Geophys. Res. Lett.*, vol. 32, no. 15, p. L15713, 2005.

[29] A. Pauling, J. Luterbacher, C. Casty, and H. Wanner, “Five hundred years of gridded high-resolution precipitation reconstructions over Europe and the connection to large-scale circulation,” *Clim. Dyn.*, vol. 26, no. 4, pp. 387–405, Mar. 2006.

[30] J. Lelieveld *et al.*, “Climate change and impacts in the Eastern Mediterranean and the Middle East,” *Clim. Change*, vol. 114, no. 3–4, pp. 667–687, Oct. 2012.

[31] J. Luterbacher *et al.*, “European summer temperatures since Roman times,” *Environ. Res. Lett.*, vol. 11, no. 2, p. 024001, Feb. 2016.

[32] S. Wagner and E. Zorita, “The influence of volcanic, solar and CO2 forcing on the temperatures in the Dalton Minimum (1790–1830): a model study,” *Clim. Dyn.*, vol. 25, no. 2–3, pp. 205–218, Aug. 2005.

[33] P. D. Jones, M. New, D. E. Parker, S. Martin, and I. G. Rigor, “Surface air temperature and its changes over the past 150 years,” *Rev. Geophys.*, vol. 37, no. 2, pp. 173–199, May 1999.

[34] H. M. Sachs, T. Webb, and D. R. Clark, “Paleoecological Transfer Functions,” *Annu. Rev. Earth Planet. Sci.*, vol. 5, no. 1, pp. 159–178, May 1977.

[35] G. J. M. Versteegh, “Solar Forcing of Climate. 2: Evidence from the Past,” *Space Sci. Rev.*, vol. 120, no. 3–4, pp. 243–286, Oct. 2005.

[36] P. D. Jones, “The Evolution of Climate Over the Last Millennium,” *Science (80-.).*, vol. 292, no. 5517, pp. 662–667, Apr. 2001.

[37] A. J. Gooday, “Benthic foraminifera (protista) as tools in deep-water palaeoceanography: Environmental influences on faunal characteristics,” 2003, pp. 1–90.

[38] M. Kucera *et al.*, “Reconstruction of sea-surface temperatures from assemblages of planktonic foraminifera: multi-technique approach based on geographically constrained calibration data sets and its application to glacial Atlantic and Pacific Oceans,” *Quat. Sci. Rev.*, vol. 24, no. 7–9, pp. 951–998, Apr. 2005.

[39] A. Rosell-Melé and E. L. McClymont, “Chapter Eleven Biomarkers as Paleoceanographic Proxies,” 2007, pp. 441–490.

[40] T. I. Eglinton and G. Eglinton, “Molecular proxies for paleoclimatology,” *Earth Planet. Sci. Lett.*, vol. 275, no. 1–2, pp. 1–16, Oct. 2008.

[41] J. Gaines, S.M., Eglinton, G., Rullko¨ tter, *Echoes of Life: What Fossil Molecules Reveal About Earth History*. Oxford: Oxford University Press, 2009.

[42] G. Eglinton and R. J. Hamilton, “Leaf Epicuticular Waxes,” *Science (80-.).*, vol. 156, no. 3780, pp. 1322–1335, Jun. 1967.

[43] J. M. Peters, K.E., Walters, C.C., Moldowan, *The biomarker guide: Biomarkers and isotopes in the environment and human history*. Cambridge University Press, 2005.

[44] P. A. Cranwell, “Chain-length distribution of n-alkanes from lake sediments in relation to post-glacial environmental change,” *Freshw. Biol.*, vol. 3, no. 3, pp. 259–265, Jun. 1973.

[45] J. G. Poynter, P. Farrimond, N. Robinson, and G. Eglinton, “Aeolian-Derived Higher Plant Lipids in the Marine Sedimentary Record: Links with Palaeoclimate,” in *Paleoclimatology and Paleometeorology: Modern and Past Patterns of Global Atmospheric Transport*, Dordrecht: Springer Netherlands, 1989, pp. 435–462.

[46] M. I. Bird *et al.*, “Terrestrial vegetation change inferred from n-alkane σ13C analysis in the marine environment,” *Geochim. Cosmochim. Acta*, vol. 59, no. 13, pp. 2853–2857, Jul. 1995.

[47] Y. Huang, L. Dupont, M. Sarnthein, J. M. Hayes, and G. Eglinton, “Mapping of C4 plant input

from North West Africa into North East Atlantic sediments," *Geochim. Cosmochim. Acta*, vol. 64, no. 20, pp. 3505–3513, Oct. 2000.

[48] Y. Huang, B. Shuman, Y. Wang, and T. Webb, "Hydrogen isotope ratios of palmitic acid in lacustrine sediments record late Quaternary climate variations," *Geology*, vol. 30, no. 12, p. 1103, 2002.

[49] K. H. Freeman and L. A. Colarusso, "Molecular and isotopic records of C4 grassland expansion in the late miocene," *Geochim. Cosmochim. Acta*, vol. 65, no. 9, pp. 1439–1454, May 2001.

[50] P. A. Cranwell, "Diagenesis of free and bound lipids in terrestrial detritus deposited in a lacustrine sediment," *Org. Geochem.*, vol. 3, no. 3, pp. 79–89, Sep. 1981.

[51] E. . Bray and E. . Evans, "Distribution of n-paraffins as a clue to recognition of source beds," *Geochim. Cosmochim. Acta*, vol. 22, no. 1, pp. 2–15, Feb. 1961.

[52] N. Ohkouchi, K. Kawamura, H. Kawahata, and A. Taira, "Latitudinal distributions of terrestrial biomarkers in the sediments from the Central Pacific," *Geochim. Cosmochim. Acta*, vol. 61, no. 9, pp. 1911–1918, 1997.

[53] Z. Wang, M. Fingas, and D. S. Page, "Oil spill identification," *J. Chromatogr. A*, vol. 843, no. 1–2, pp. 369–411, May 1999.

[54] J. Poynter and G. Eglington, "Molecular composition of three sediments from hole 717C: the Bengal Fan," in *Proc., scientific results, ODP, Leg. 116, distal Bengal Fan*, 1990, pp. 155–161.

[55] K. Kouli *et al.*, "Late postglacial paleoenvironmental change in the northeastern Mediterranean region: Combined palynological and molecular biomarker evidence," *Quat. Int.*, vol. 261, pp. 118–127, 2012.

[56] I. T. Marlowe, J. C. Green, A. C. Neal, S. C. Brassell, G. Eglinton, and P. A. Course, "Long chain (n -C 37 –C 39) alkenones in the Prymnesiophyceae. Distribution of alkenones and other lipids and their taxonomic significance," *Br. Phycol. J.*, vol. 19, no. 3, pp. 203–216, Sep. 1984.

[57] J. K. Volkman, "A review of sterol markers for marine and terrigenous organic matter," *Org. Geochem.*, vol. 9, no. 2, pp. 83–99, Jan. 1986.

[58] S. W. Rampen, S. Schouten, E. Koning, G.-J. A. Brummer, and J. S. Sinninghe Damsté, "A 90 kyr upwelling record from the northwestern Indian Ocean using a novel long-chain diol index," *Earth Planet. Sci. Lett.*, vol. 276, no. 1–2, pp. 207–213, Nov. 2008.

[59] M. Rodrigo-Gámiz, F. Martínez-Ruiz, S. W. Rampen, S. Schouten, and J. S. Sinninghe Damsté, "Sea surface temperature variations in the western Mediterranean Sea over the last 20 kyr: A dual-organic proxy (U K′ 37 and LDI) approach," *Paleoceanography*, vol. 29, no. 2, pp. 87–98, Feb. 2014.

[60] D. J. Repeta, "Carotenoid diagenesis in recent marine sediments: II. Degradation of fucoxanthin to loliolide," *Geochim. Cosmochim. Acta*, vol. 53, no. 3, pp. 699–707, Mar. 1989.

[61] J. K. Volkman, S. M. Barrett, and S. I. Blackburn, "Eustigmatophyte microalgae are potential sources of C29 sterols, C22–C28 n-alcohols and C28–C32 n-alkyl diols in freshwater environments," *Org. Geochem.*, vol. 30, no. 5, pp. 307–318, May 1999.

[62] D. Menzel, P. F. van Bergen, S. Schouten, and J. S. Sinninghe Damsté, "Reconstruction of

changes in export productivity during Pliocene sapropel deposition: a biomarker approach," *Palaeogeogr. Palaeoclimatol. Palaeoecol.*, vol. 190, pp. 273–287, Jan. 2003.

[63] J. K. Volkman, G. Eglinton, E. D. S. Corner, and T. E. V. Forsberg, "Long-chain alkenes and alkenones in the marine coccolithophorid Emiliania huxleyi," *Phytochemistry*, vol. 19, no. 12, pp. 2619–2622, Jan. 1980.

[64] J. K. Volkman, S. M. Barrerr, S. I. Blackburn, and E. L. Sikes, "Alkenones in Gephyrocapsa oceanica: Implications for studies of paleoclimate," *Geochim. Cosmochim. Acta*, vol. 59, no. 3, pp. 513–520, Feb. 1995.

[65] M. H. Conte, A. Thompson, D. Lesley, and R. P. Harris, "Genetic and Physiological Influences on the Alkenone/Alkenoate Versus Growth Temperature Relationship in Emiliania huxleyi and Gephyrocapsa Oceanica," *Geochim. Cosmochim. Acta*, vol. 62, no. 1, pp. 51–68, Jan. 1998.

[66] S. C. Brassell *et al.*, "Palaeoclimatic signals recognized by chemometric treatment of molecular stratigraphic data," *Org. Geochem.*, vol. 10, no. 4–6, pp. 649–660, Jan. 1986.

[67] F. G. Prahl and S. G. Wakeham, "Calibration of unsaturation patterns in long-chain ketone compositions for palaeotemperature assessment," *Nature*, vol. 330, no. 6146, pp. 367–369, Nov. 1987.

[68] P. J. Müller, G. Kirst, G. Ruhland, I. von Storch, and A. Rosell-Melé, "Calibration of the alkenone paleotemperature index U37K′ based on core-tops from the eastern South Atlantic and the global ocean (60°N-60°S)," *Geochim. Cosmochim. Acta*, vol. 62, no. 10, pp. 1757–1772, May 1998.

[69] M. Conte *et al.*, "Global temperature calibration of the alkenone unsaturation index (Uk37) in surface waters and comparison with surface sediments," *Geochemistry Geophys. Geosystems*, vol. 7, no. 2, pp. 1525–2027, 2006.

[70] Y. Ternois, M.-A. Sicre, A. Boireau, M. H. Conte, and G. E, "Evaluation of long-chain alkenones as paleo-temperature indicators in the Mediterranean Sea," *Deep Sea Res. Part I Oceanogr. Res. Pap.*, vol. 44, no. 2, pp. 271–286, Feb. 1997.

[71] I. Bentaleb *et al.*, "The C37 alkenone record of seawater temperature during seasonal thermocline stratification," *Mar. Chem.*, vol. 64, no. 4, pp. 301–313, Apr. 1999.

[72] M. . Conte, J. . Weber, L. . King, and S. . Wakeham, "The alkenone temperature signal in western North Atlantic surface waters," *Geochim. Cosmochim. Acta*, vol. 65, no. 23, pp. 4275–4287, Dec. 2001.

[73] F. G. Prahl, B. N. Popp, D. M. Karl, and M. A. Sparrow, "Ecology and biogeochemistry of alkenone production at Station ALOHA," *Deep Sea Res. Part I Oceanogr. Res. Pap.*, vol. 52, no. 5, pp. 699–719, May 2005.

[74] E. L. Sikes, J. K. Volkman, L. G. Robertson, and J.-J. Pichon, "Alkenones and alkenes in surface waters and sediments of the Southern Ocean: Implications for paleotemperature estimation in polar regions," *Geochim. Cosmochim. Acta*, vol. 61, no. 7, pp. 1495–1505, Apr. 1997.

[75] J. K. Volkman, "Ecological and environmental factors affecting alkenone distributions in seawater and sediments," *Geochemistry, Geophys. Geosystems*, vol. 1, no. 9, p. n/a-n/a, Sep. 2000.

[76] F. . Prahl, C. . Pilskaln, and M. . Sparrow, "Seasonal record for alkenones in sedimentary particles from the Gulf of Maine," *Deep Sea Res. Part I Oceanogr. Res. Pap.*, vol. 48, no. 2, pp. 515–528,

Feb. 2001.

[77] B. N. Popp, F. G. Prahl, R. J. Wallsgrove, and J. Tanimoto, “Seasonal patterns of alkenone production in the subtropical oligotrophic North Pacific,” *Paleoceanography*, vol. 21, no. 1, p. n/a-n/a, Mar. 2006.

[78] M.-Y. Sun and S. G. Wakeham, “Molecular evidence for degradation and preservation of organic matter in the anoxic Black Sea Basin,” *Geochim. Cosmochim. Acta*, vol. 58, no. 16, pp. 3395–3406, Aug. 1994.

[79] M. J. L. Hoefs, W. I. C. Rijpstra, and J. S. Sinninghe Damsté, “The influence of oxic degradation on the sedimentary biomarker record I: evidence from Madeira Abyssal Plain turbidites,” *Geochim. Cosmochim. Acta*, vol. 66, no. 15, pp. 2719–2735, Aug. 2002.

[80] C. Gong and D. J. Hollander, “Evidence for differential degradation of alkenones under contrasting bottom water oxygen conditions: implication for paleotemperature reconstruction,” *Geochim. Cosmochim. Acta*, vol. 63, no. 3–4, pp. 405–411, Feb. 1999.

[81] J.-F. Rontani, N. Zabeti, and S. G. Wakeham, “The fate of marine lipids: Biotic vs. abiotic degradation of particulate sterols and alkenones in the Northwestern Mediterranean Sea,” *Mar. Chem.*, vol. 113, no. 1–2, pp. 9–18, Jan. 2009.

[82] J.-F. Rontani, J.-C. Marty, J.-C. Miquel, and J. K. Volkman, “Free radical oxidation (autoxidation) of alkenones and other microalgal lipids in seawater,” *Org. Geochem.*, vol. 37, no. 3, pp. 354–368, Mar. 2006.

[83] J.-H. Kim *et al.*, “An experimental field study to test the stability of lipids used for the TEX86 and palaeothermometers,” *Geochim. Cosmochim. Acta*, vol. 73, no. 10, pp. 2888–2898, May 2009.

[84] T. D. Herbert, “6.15 - Alkenone Paleotemperature Determinations,” pp. 391–432, 2003.

[85] J. Volkman, “Sterols in microorganisms,” *Appl. Microbiol. Biotechnol.*, vol. 60, no. 5, pp. 495–506, Jan. 2003.

[86] K. Grice and C. Eiserbeck, *The Analysis and Application of Biomarkers*, 12th ed., vol. 12. Elsevier Ltd., 2013.

[87] S. K. Samanta, O. V Singh, and R. K. Jain, “Polycyclic aromatic hydrocarbons: environmental pollution and bioremediation,” *Trends Biotechnol.*, vol. 20, no. 6, pp. 243–248, Jun. 2002.

[88] B. R. T. Simoneit, “Organic matter of the troposphere—III. Characterization and sources of petroleum and pyrogenic residues in aerosols over the western united states,” *Atmos. Environ.*, vol. 18, no. 1, pp. 51–67, Jan. 1984.

[89] S. A. Bouloubassi I, “Investigation of anthropogenic and natural organic inputs in estuarine sediments using hydrocarbon markers (nah, lab, pah),” *Oceanol. Acta*, vol. 16, no. 2, pp. 145–161, 1993.

[90] D. L. Leister and J. E. Baker, “Atmospheric deposition of organic contaminants to the chesapeake bay,” *Atmos. Environ.*, vol. 28, no. 8, pp. 1499–1520, May 1994.

[91] I. Tolosa, J. M. Bayona, and J. Albaigés, “Aliphatic and Polycyclic Aromatic Hydrocarbons and Sulfur/Oxygen Derivatives in Northwestern Mediterranean Sediments: Spatial and Temporal Variability, Fluxes, and Budgets,” *Environ. Sci. Technol.*, vol. 30, no. 8, pp. 2495–2503, Jan.

1996.

[92] M. Tsapakis, M. Apostolaki, S. Eisenreich, and E. G. Stephanou, “Atmospheric Deposition and Marine Sedimentation Fluxes of Polycyclic Aromatic Hydrocarbons in the Eastern Mediterranean Basin,” *Environ. Sci. Technol.*, vol. 40, no. 16, pp. 4922–4927, Aug. 2006.

[93] F. G. Prahl and R. Carpenter, “The role of zooplankton fecal pellets in the sedimentation of polycyclic aromatic hydrocarbons in Dabob Bay, Washington,” *Geochim. Cosmochim. Acta*, vol. 43, no. 12, pp. 1959–1972, Dec. 1979.

[94] E. Lipiatou *et al.*, “Mass budget and dynamics of polycyclic aromatic hydrocarbons in the Mediterranean Sea,” *Deep Sea Res. Part II Top. Stud. Oceanogr.*, vol. 44, no. 3–4, pp. 881–905, 1997.

[95] J. Dachs, R. Lohmann, W. A. Ockenden, L. Méjanelle, S. J. Eisenreich, and K. C. Jones, “Oceanic Biogeochemical Controls on Global Dynamics of Persistent Organic Pollutants,” *Environ. Sci. Technol.*, vol. 36, no. 20, pp. 4229–4237, Oct. 2002.

[96] I. Bouloubassi, L. Méjanelle, R. Pete, J. Fillaux, A. Lorre, and V. Point, “PAH transport by sinking particles in the open Mediterranean Sea: A 1 year sediment trap study,” *Mar. Pollut. Bull.*, vol. 52, no. 5, pp. 560–571, May 2006.

[97] R. Deyme *et al.*, “Vertical fluxes of aromatic and aliphatic hydrocarbons in the Northwestern Mediterranean Sea,” *Environ. Pollut.*, vol. 159, no. 12, pp. 3681–3691, Dec. 2011.

[98] H. Kontoyiannis, “Observations on the circulation of the Saronikos Gulf: A Mediterranean embayment sea border of Athens, Greece,” *J. Geophys. Res. Ocean.*, vol. 115, no. 6, pp. 1–23, 2010.

[99] A. Pavlidou, H. Kontoyiannis, N. Zarokanelos, I. Hatzianestis, G. Assimakopoulou, and R. Psyllidou-Giouranovits, “Seasonal and Spatial Nutrient Dynamics in Saronikos Gulf: The Impact of Sewage Effluents from Athens Sewage Treatment Plant,” in *Eutrophication: Causes, Consequences and Control*, Dordrecht: Springer Netherlands, 2014, pp. 111–130.

[100] M. Dassenakis, V. Paraskevopoulou, C. Cartalis, N. Adaktilou, and K. Katsiabani, “Remote sensing in coastal water monitoring: Applications in the eastern Mediterranean Sea (IUPAC Technical Report),” *Pure Appl. Chem.*, vol. 84, no. 2, pp. 335–375, Dec. 2011.

[101] P. D. Kalabokas, L. G. Viras, J. G. Bartzis, and C. C. Repapis, “Mediterranean rural ozone characteristics around the urban area of Athens,” *Atmos. Environ.*, vol. 34, no. 29–30, pp. 5199–5208, Jan. 2000.

[102] V. Kapsimalis *et al.*, “Organic contamination of surface sediments in the metropolitan coastal zone of Athens, Greece: Sources, degree, and ecological risk,” *Mar. Pollut. Bull.*, vol. 80, no. 1–2, pp. 312–324, Mar. 2014.

[103] C. Vasilakos *et al.*, “Temporal determination of heavy metals in PM2.5 aerosols in a suburban site of Athens, Greece,” *J. Atmos. Chem.*, vol. 57, no. 1, pp. 1–17, Apr. 2007.

[104] S. Xenarios and K. Bithas, “Valuating the Receiving Waters of Urban Wastewater Systems through a Stakeholder-based Approach,” *Int. J. Water Resour. Dev.*, vol. 25, no. 1, pp. 123–140, Mar. 2009.

[105] F. Botsou and I. Hatzianestis, “Polycyclic aromatic hydrocarbons (PAHs) in marine sediments of

the Hellenic coastal zone, eastern Mediterranean: levels, sources and toxicological significance," *J. Soils Sediments*, vol. 12, no. 2, pp. 265–277, Feb. 2012.

[106] I. Hatzianestis, N. Rori, E. Sklivagou, and F. Rigas, "Pah Profiles in Dated Sediment Cores From Elefsis Bay , Greece Pah Profiles in Dated Sediment Cores From Elefsis Bay , Greece," vol. 13, no. 11, pp. 1253–1257, 2004.

[107] E. Sklivagou, S. P. Varnavas, I. Hatzianestis, and G. Kanias, "Assessment of Aliphatic and Polycyclic Aromatic Hydrocarbons and Trace Elements in Coastal Sediments of the Saronikos Gulf, Greece (Eastern Mediterranean)," *Mar. Georesources Geotechnol.*, vol. 26, no. 4, pp. 372–393, Dec. 2008.

[108] T. Hopkins, L. Coachman, and R. Edwards, "Seasonal changes in Elefsis Bay," in *XXIV Congres-Assemblee Pleniere du Monaco (CIESM), Greece*, 1974.

[109] S. Pantazidou, A. Kapniaris, A. Katsiri, and A. Christidis, "Pollutant trends and hazard ranking in Elefsis Bay," *Desalination*, vol. 210, pp. 69–82, 2007.

[110] T. Vlahogianni, M. Dassenakis, M. J. Scoullos, and A. Valavanidis, "Integrated use of biomarkers (superoxide dismutase, catalase and lipid peroxidation) in mussels Mytilus galloprovincialis for assessing heavy metals' pollution in coastal areas from the Saronikos Gulf of Greece," *Mar. Pollut. Bull.*, vol. 54, no. 9, pp. 1361–1371, Sep. 2007.

[111] N. Friligos, "Seasonal variations of nutrients around the sewage outfall in the Saronikos Gulf," *Thalass. Yugosl*, vol. 12, pp. 441–453, 1973.

[112] C. Yannopoulos, "The annual regeneration of the Elefsis Bay zooplankton ecosystem, Saronikos Gulf," *Rapp Comm Int Mer Medit*, vol. 5, pp. 109–111, 1976.

[113] N. Friligos, "Nutrient and oxygen conditions in the Elefsis bay, an intermittently anoxic Mediterranean basin," *Toxicol. Environ. Chem.*, vol. 19, no. 3–4, pp. 179–186, Mar. 1989.

[114] N. Friligos, "Influence of industries and sewage on the pollution of Elefsis Bay (January 21st, 1974)," *Rer Int d'Ocean Med*, vol. 55, pp. 3–11, 1979.

[115] N. Friligos, "Enrichment by inorganic nutrients and oxygen utilization rates in Elefsis Bay (1973–1976)," *Mar. Pollut. Bull.*, vol. 12, no. 12, pp. 431–436, Dec. 1981.

[116] N. Friligos, "Some consequences of the decomposition of organic matter in the Elefsis bay, an anoxic basin," *Mar. Pollut. Bull.*, vol. 13, no. 3, pp. 103–106, Mar. 1982.

[117] N. Friligos, "Preliminary observations on nutrient cycling and a stoichiometric model for elefsis bay, Greece," *Mar. Environ. Res.*, vol. 8, no. 4, pp. 197–213, Apr. 1983.

[118] M. Scoulos, "Chemical studies of the gulf of Elefsis, Greece," 1979.

[119] A. Pavlidou *et al.*, "Biogeochemical Characteristics in the Elefsis Bay (Aegean Sea, Eastern Mediterranean) in Relation to Anoxia and Climate Changes," in *Biogeochemical Characteristics in the Elefsis Bay (Aegean Sea, Easterrn Mediterranean) in Relation to Anoxia and Climate Changes*, vol. 22, 2010, pp. 161–201.

[120] M. J. Scoullos, "Lead in coastal sediments: The case of the elefsis gulf, Greece," *Sci. Total Environ.*, vol. 49, pp. 199–219, Mar. 1986.

[121] A. Valavanidis, T. Vlachogianni, S. Triantafillaki, M. Dassenakis, F. Androutsos, and M. Scoullos, “Polycyclic aromatic hydrocarbons in surface seawater and in indigenous mussels (Mytilus galloprovincialis) from coastal areas of the Saronikos Gulf (Greece),” *Estuar. Coast. Shelf Sci.*, vol. 79, no. 4, pp. 733–739, Sep. 2008.

[122] M. J. Scoullos, A. Sakellari, K. Giannopoulou, V. Paraskevopoulou, and M. Dassenakis, “Dissolved and particulate trace metal levels in the Saronikos Gulf, Greece, in 2004. The impact of the primary Wastewater Treatment Plant of Psittalia,” *Desalination*, vol. 210, no. 1–3, pp. 98–109, Jun. 2007.

[123] J. Nieuwenhuize, Y. E. . Maas, and J. J. Middelburg, “Rapid analysis of organic carbon and nitrogen in particulate materials,” *Mar. Chem.*, vol. 45, no. 3, pp. 217–224, Feb. 1994.

[124] A. Gogou, I. Bouloubassi, V. Lykousis, M. Arnaboldi, P. Gaitani, and P. A. Meyers, “Organic geochemical evidence of Late Glacial-Holocene climate instability in the North Aegean Sea,” *Palaeogeogr. Palaeoclimatol. Palaeoecol.*, vol. 256, no. 1–2, pp. 1–20, 2007.

[125] A. J. Shusterman, P. G. McDougal, and A. Glasfeld, “Dry-Column Flash Chromatography,” *J. Chem. Educ.*, vol. 74, no. 10, p. 1222, Oct. 1997.

[126] R. Pedrosa-Pàmies *et al.*, “Composition and sources of sedimentary organic matter in the deep Eastern Mediterranean Sea,” *Biogeosciences Discuss.*, vol. 12, no. 13, pp. 9935–9989, 2015.

[127] A. Gogou *et al.*, “Climate variability and socio-environmental changes in the northern Aegean (NE Mediterranean) during the last 1500 years,” *Quat. Sci. Rev.*, vol. 136, pp. 209–228, 2016.

[128] K.-U. Hinrichs, R. . Schneider, P. . Müller, and J. Rullkötter, “A biomarker perspective on paleoproductivity variations in two Late Quaternary sediment sections from the Southeast Atlantic Ocean,” *Org. Geochem.*, vol. 30, no. 5, pp. 341–366, May 1999.

[129] D. Strong *et al.*, “A new regional, mid-Holocene palaeoprecipitation signal of the Asian Summer Monsoon,” *Quat. Sci. Rev.*, vol. 78, pp. 65–76, Oct. 2013.

[130] X. Ouyang, F. Guo, and H. Bu, “Lipid biomarkers and pertinent indices from aquatic environment record paleoclimate and paleoenvironment changes,” *Quat. Sci. Rev.*, vol. 123, pp. 180–192, Sep. 2015.

[131] S. C. BRASSELL, G. EGLINTON, J. R. MAXWELL, and R. P. PHILP, “Natural Background of Alkanes in the Aquatic Environment,” in *Aquatic Pollutants*, Elsevier, 1978, pp. 69–86.

[132] B. R. T. Simoneit, J. N. Cardoso, and N. Robinson, “An assessment of the origin and composition of higher molecular weight organic matter in aerosols over Amazonia,” *Chemosphere*, vol. 21, no. 10–11, pp. 1285–1301, Jan. 1990.

[133] T. A. T. Aboul-Kassim and B. R. T. Simoneit, “Petroleum hydrocarbon fingerprinting and sediment transport assessed by molecular biomarker and multivariate statistical analyses in the Eastern Harbour of Alexandria, Egypt,” *Mar. Pollut. Bull.*, vol. 30, no. 1, pp. 63–73, Jan. 1995.

[134] M. Gough and S. Rowland, “Characterization of unresolved complex mixtures of hydrocarbons in petroleum,” *Nature*, vol. 344, pp. 648–650, 1990.

[135] A. Scarlett, T. S. Galloway, and S. J. Rowland, “Chronic toxicity of unresolved complex mixtures (UCM) of hydrocarbons in marine sediments,” *J. Soils Sediments*, vol. 7, no. 4, pp. 200–206, Aug. 2007.

[136] C. Parinos, A. Gogou, I. Bouloubassi, S. Stavrakakis, E. Plakidi, and I. Hatzianestis, “Sources and downward fluxes of polycyclic aromatic hydrocarbons in the open southwestern Black Sea,” *Org. Geochem.*, vol. 57, pp. 65–75, 2013.

[137] A. K. Singh, R. K. Chaudhuri, and S. Ghosal, “Chemical Constituents of Gentianaceae XX: Natural Occurrence of (—)-Loliolide in Canscora Decussata,” *J. Pharm. Sci.*, vol. 65, no. 10, pp. 1549–1551, Oct. 1976.

[138] D. J. Repeta, “Carotenoid diagenesis in recent marine sediments: II. Degradation of fucoxanthin to loliolide,” *Geochim. Cosmochim. Acta*, vol. 53, no. 3, pp. 699–707, Mar. 1989.

[139] S. Isoe, S. B. Hyeon, S. Katsumura, and T. Sakan, “Photo-oxygenation of carotenoids. II. The absolute configuration of loliolide and dihydroactinidiolide.,” *Tetrahedron Lett.*, vol. 13, no. 25, pp. 2517–2520, 1972.

[140] J. Klok, M. Baas, H. C. Cox, J. W. de Leeuw, and P. A. Schenck, “Loliolides and dihydroactinidiolide in a recent marine sediment probably indicate a major transformation pathway of carotenoids,” *Tetrahedron Lett.*, vol. 25, no. 48, pp. 5577–5580, Jan. 1984.

[141] J. O. Grimalt *et al.*, “Modifications of the C 37 alkenone and alkenoate composition in the water column and sediment: Possible implications for sea surface temperature estimates in paleoceanography,” *Geochemistry, Geophys. Geosystems*, vol. 1, no. 11, p. n/a-n/a, Nov. 2000.

[142] M. V. Triantaphyllou, “Coccolithophore export production and response to seasonal surface water variability in the oligotrophic Cretan Sea (NE Mediterranean),” *Micropaleontology*, vol. 50, no. Suppl_1, pp. 127–144, Dec. 2004.

[143] E. Malinverno, M. V. Triantaphyllou, S. Stavrakakis, P. Ziveri, and V. Lykousis, “Seasonal and spatial variability of coccolithophore export production at the South-Western margin of Crete (Eastern Mediterranean),” *Mar. Micropaleontol.*, vol. 71, no. 3–4, pp. 131–147, May 2009.

[144] J. S. Latimer and J. Zheng, “The sources, transport, and fate of PAHs in the marine environment.,” in *PAHs: An Ecotoxicological Perspective.*, John Wiley & Sons, Ltd., West Sussex, England, 2003, pp. 9–33.

[145] T. Ramdahl, “Retene—a molecular marker of wood combustion in ambient air,” *Nature*, vol. 306, no. 5943, pp. 580–582, Dec. 1983.

[146] M. B. Yunker and R. W. Macdonald, “Alkane and PAH depositional history, sources and fluxes in sediments from the Fraser River Basin and Strait of Georgia, Canada,” *Org. Geochem.*, vol. 34, no. 10, pp. 1429–1454, Oct. 2003.

[147] S. Azoury *et al.*, “Historical Records of Mercury, Lead, and Polycyclic Aromatic Hydrocarbons Depositions in a Dated Sediment Core from the Eastern Mediterranean,” *Environ. Sci. Technol.*, vol. 47, no. 13, pp. 7101–7109, Jul. 2013.

[148] A. Papaioannou *et al.*, “A high resolution multidisciplinary study of palaeoenvironmental changes in the Gulf of Elefsis, Attica, Greece during the last 300 years,” in *GSG2019*, 2019.

[149] A. Papaioannou, A.; Kouli, K.; Parinos, C.; Dimiza, M.; Triantaphyllou, M.; Dasenakis, M.; Miaritis, K.; Gogou, “A 300 years old high resolution palaeoenvironmental record from the Gulf of Elefsis, Attica, South Greece,” 2018.

[150] M. V. Triantaphyllou *et al.*, “Late Glacial–Holocene ecostratigraphy of the south-eastern Aegean

Sea, based on plankton and pollen assemblages," *Geo-Marine Lett.*, vol. 29, no. 4, pp. 249–267, Aug. 2009.

[151] M. V. Triantaphyllou *et al.*, "Evidence for a warm and humid Mid-Holocene episode in the Aegean and northern Levantine Seas (Greece, NE Mediterranean)," *Reg. Environ. Chang.*, vol. 14, no. 5, pp. 1697–1712, 2014.

[152] E. Sklivagou, S. P. Varnavas, and J. Hatzianestis, "Aliphatic and polycyclic aromatic hydrocarbons in surface sediments from Elefsis Bay, Greece (Eastern Mediterranean)," *Toxicol. Environ. Chem.*, vol. 79, no. 3–4, pp. 195–210, Feb. 2001.

[153] J. W. Collister, G. Rieley, B. Stern, G. Eglinton, and B. Fry, "Compound-specific δ 13C analyses of leaf lipids from plants with differing carbon dioxide metabolisms," *Org. Geochem.*, vol. 21, no. 6–7, pp. 619–627, Jun. 1994.

[154] P. H. Bethell, L. J. Goad, R. P. Evershed, and J. Ottaway, "The Study of Molecular Markers of Human Activity: The Use of Coprostanol in the Soil as an Indicator of Human Faecal Material," *J. Archaeol. Sci.*, vol. 21, no. 5, pp. 619–632, Sep. 1994.

[155] Β. Πατρώνης, *Ελληνική Οικονομική Ιστορία*. 2015.

[156] P. Fernández, R. M. Vilanova, C. Martínez, P. Appleby, and J. O. Grimalt, "The Historical Record of Atmospheric Pyrolytic Pollution over Europe Registered in the Sedimentary PAH from Remote Mountain Lakes," *Environ. Sci. Technol.*, vol. 34, no. 10, pp. 1906–1913, May 2000.

[157] A. L. C. Lima, T. I. Eglinton, and C. M. Reddy, "High-Resolution Record of Pyrogenic Polycyclic Aromatic Hydrocarbon Deposition during the 20th Century," *Environ. Sci. Technol.*, vol. 37, no. 1, pp. 53–61, Jan. 2003.

[158] C. Gallon, A. Tessier, C. Gobeil, and L. Beaudin, "Sources and chronology of atmospheric lead deposition to a Canadian Shield lake: Inferences from Pb isotopes and PAH profiles," *Geochim. Cosmochim. Acta*, vol. 69, no. 13, pp. 3199–3210, Jul. 2005.

[159] A. R. Schneider, H. M. Stapleton, J. Cornwell, and J. E. Baker, "Recent Declines in PAH, PCB, and Toxaphene Levels in the Northern Great Lakes As Determined from High Resolution Sediment Cores," *Environ. Sci. Technol.*, vol. 35, no. 19, pp. 3809–3815, Oct. 2001.

[160] M. F. Simcik *et al.*, "Atmospheric Loading of Polycyclic Aromatic Hydrocarbons to Lake Michigan as Recorded in the Sediments," *Environ. Sci. Technol.*, vol. 30, no. 10, pp. 3039–3046, Jan. 1996.

[161] P. C. Van Metre and B. J. Mahler, "Contaminant Trends in Reservoir Sediment Cores as Records of Influent Stream Quality," *Environ. Sci. Technol.*, vol. 38, no. 11, pp. 2978–2986, Jun. 2004.

[162] S. G. Wakeham, J. Forrest, C. A. Masiello, Y. Gélinas, C. R. Alexander, and P. R. Leavitt, "Hydrocarbons in Lake Washington Sediments. A 25-Year Retrospective in an Urban Lake," *Environ. Sci. Technol.*, vol. 38, no. 2, pp. 431–439, Jan. 2004.

[163] S. Usenko, D. H. Landers, P. G. Appleby, and S. L. Simonich, "Current and Historical Deposition of PBDEs, Pesticides, PCBs, and PAHs to Rocky Mountain National Park," *Environ. Sci. Technol.*, vol. 41, no. 21, pp. 7235–7241, Nov. 2007.

[164] H. Lu *et al.*, "PAHs in the Fraser River basin: A critical appraisal of PAH ratios as indicators of PAH source and composition," *Org. Geochem.*, vol. 223, no. 4, pp. 489–515, 2002.